

Millimeter-Wave and Terahertz Transceivers in SiGe BiCMOS Technologies

Dietmar Kissinger¹, Senior Member, IEEE, Gerhard Kahmen², Senior Member, IEEE,
and Robert Weigel³, Fellow, IEEE

(Invited Paper)

Abstract—This invited paper reviews the progress of silicon–germanium (SiGe) bipolar-complementary metal–oxide–semiconductor (BiCMOS) technology-based integrated circuits (ICs) during the last two decades. Focus is set on various transceiver (TRX) realizations in the millimeter-wave range from 60 GHz and at terahertz (THz) frequencies above 300 GHz. This article discusses the development of SiGe technologies and ICs with the latter focusing on the commercially most important applications of radar and beyond 5G wireless communications. A variety of examples ranging from 77-GHz automotive radar to THz sensing as well as the beginnings of 60-GHz wireless communication up to THz chipsets for 100-Gb/s data transmission are recapitulated. This article closes with an outlook on emerging fields of research for future advancement of SiGe TRX performance.

Index Terms—BiCMOS ICs, data communication, heterojunction bipolar transistors (HBTs), millimeter-wave circuits, radar, submillimeter-wave circuits, transceivers (TRXs).

I. INTRODUCTION

SILICON is the most mature and advanced manufacturing technology in the electronics industry. From the electrical point of view, it is not the best semiconductor material with respect to intrinsic carrier density or mobility if compared to Ge or III–V semiconductors. However, the existence of a natural oxide (SiO₂) for masking and high-quality thin layers together with the superior handling properties during manufacturing enabled the unprecedented success of silicon as the material of choice for the semiconductor industry.

The properties of millimeter-wave and terahertz (THz) integrated circuits (ICs) are fundamentally affected by the basic characteristics of the active devices. The transit frequency f_t , defined as the frequency where the short-circuited small-signal current gain equals 1, significantly determines the

performance, such as the gate delay τ_{CML} and phase noise of fast (current-mode) logic circuits. The maximum frequency of oscillation f_{max} , defined as the point where the unilateral active device power gain becomes unity, determines the bandwidth and high-frequency properties of tuned RF blocks, such as amplifiers and oscillators. This f_{max} is closely linked to the transconductance g_m , which is essential to achieve high gain and linearity for analog/mixed-signal circuits, e.g., if feedback topologies are applied. Furthermore, the breakdown voltage BV_{CE0} directly determines the power handling capabilities of the transistor device. Finally, parameters, such as the base resistance R_B and the $1/f$ flicker noise corner, have a direct impact on the circuits noise. Here, the goal of device engineering is to maximize f_t , f_{max} , g_m , and BV_{CE0} while minimizing R_B and $1/f$.

The first mention of silicon–germanium (SiGe) devices was actually in the original patent for the bipolar transistor in 1948, while the idea of a SiGe heterojunction bipolar transistor (HBT) was first discussed, with a description of the physics, by Kroemer [1], [2]. However, the successful implementation was delayed until 1975 when Kasper *et al.* [3] demonstrated the growth of a 1-D SiGe superlattice by epitaxy. Thenceforth, the developments toward practical SiGe devices have been exceptionally rapid and the combination of SiGe HBT features with high-density CMOS logic resulted in today’s bipolar-complementary metal–oxide–semiconductor (BiCMOS) technologies. Here, SiGe delivers high output powers, high-frequency gain, and low noise leading to improved signal-to-noise ratios, while CMOS provides the logic functions required for signal conditioning and processing. Depending on the production volume, the mask and wafer costs, and the die size, the BiCMOS combination may be more costly than advanced CMOS technologies, but for many special applications, the performance of BiCMOS exceeds that of CMOS alone. In the end, for specific applications, it depends on the business case whether CMOS outperforms BiCMOS and whether BiCMOS outperforms III–V technologies or not.

This article focuses on the commercially most important applications of radar and wireless communications. While 24-GHz automotive radar and *Ka*-band satellite communication (26–40 GHz) have been around for years, only the recent launch of 5G around 28/39 GHz has triggered the

Manuscript received May 11, 2021; revised June 25, 2021; accepted June 27, 2021. Date of publication July 28, 2021; date of current version October 5, 2021. (Corresponding author: Dietmar Kissinger.)

Dietmar Kissinger is with the Institute of Electronic Devices and Circuits, Ulm University, 89081 Ulm, Germany (e-mail: kissinger@ieee.org).

Gerhard Kahmen is with IHP—Leibniz-Institut für innovative Mikroelektronik, 15236 Frankfurt (Oder), Germany (e-mail: kahmen@ihp-microelectronics.com).

Robert Weigel is with the Institute for Electronics Engineering, University of Erlangen-Nuremberg, 91058 Erlangen, Germany (e-mail: r.weigel@ieee.org).

Color versions of one or more figures in this article are available at <https://doi.org/10.1109/TMTT.2021.3095235>.

Digital Object Identifier 10.1109/TMTT.2021.3095235

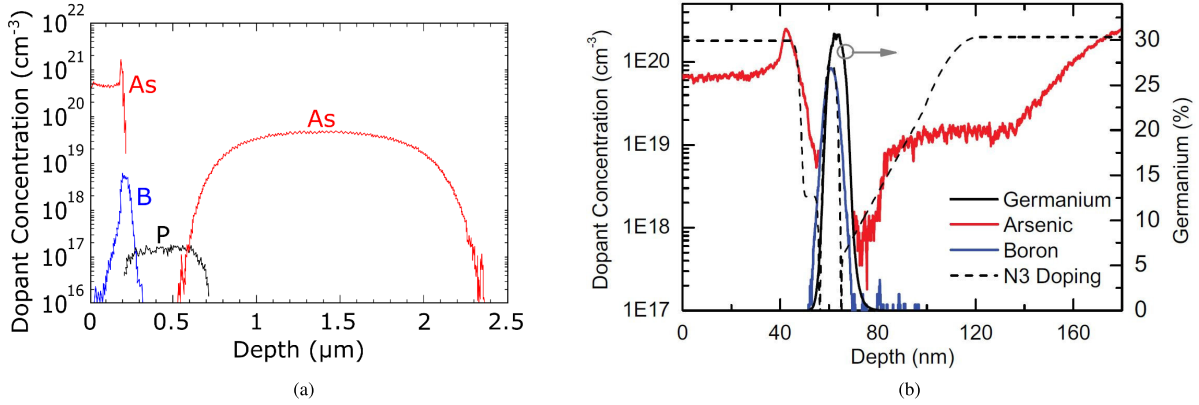


Fig. 1. Doping profile of a typical (a) homojunction bipolar transistor after [18] and (b) heterojunction bipolar transistor as reported in [19].

millimeter-wave hype. The technology relies on phased arrays with coherent combination of multiple channels to mitigate high free-space path loss [4]. Beyond radar and communications, SiGe has also been employed in radiometers [5]–[7] and active imagers. A comprehensive overview on THz imaging in silicon can be found in [8]. In addition, SiGe has successfully been used in gas spectroscopy [9]–[11] and biosensing [12]–[17].

II. SILICON–GERMANIUM TECHNOLOGY

A. SiGe HBT Fundamentals

A bipolar transistor is a device where current flow is dominated by minority carriers. These are injected from the emitter to the base through the forward-biased emitter–base junction. The minority carriers are swept through the base and then carried through the reverse-biased base–collector junction by the large electric field in this region [20]. In the following, some elementary equations of bipolar transistors are reviewed [21] to explain the fundamental advantages of the HBT principle.

The emitter-injection efficiency γ , dominating the current gain β of the device, describes the ratio of minority carriers (electrons) injected from emitter to base to the minority carriers (holes) injected from base to emitter, which is expressed as

$$1/\gamma = 1 + 1/\beta = 1 + \frac{D_p W_B N_A}{D_n L_p N_D} \quad (1)$$

where N_D is the donor dopant concentration of the n-type emitter, N_A is the acceptor concentration of the p-type base, and D_p and D_n are the corresponding diffusion constants. The emitter-injection efficiency should be as close to 1 as possible to achieve a large current gain β . Furthermore, the transit frequency f_t of the bipolar transistor is given by

$$\frac{1}{2\pi f_t} = \tau_B + \frac{C_{bej}}{g_m} + \frac{C_{bcj}}{g_m} \quad \text{with} \quad \tau_B = \frac{W_B^2}{2D_n} \quad (2)$$

where τ_B is the electron transit time through the base. Finally, the base resistance R_B of a bipolar transistor is given by

$$R_B = \frac{A}{q\mu_p N_A W_B}. \quad (3)$$

As can be seen from (1) and (2), an emitter doping N_D exceeding the base doping N_A by orders of magnitude is essential, and at the same time, a base width W_B as low as possible is required to increase the current gain β and the transit frequency f_t . On the other hand, a large base width W_B and high base doping N_A are required to achieve a low base resistance resulting in a low RC time constant and less base noise. This problem cannot be resolved in a standard homojunction bipolar transistor device. The key to overcome this contradiction is the principle of a heterojunction bipolar device, which was theoretically introduced by Kroemer [2]. The basic idea is to add germanium into the base lowering the bandgap of the base compared to the bandgap of the emitter and the collector [22]. As the Fermi energy level within emitter, base, and collector is the same, a lowered barrier in the conduction band compared to the barrier in the valence band is the result of Si emitter–Si_xGe_{1-x} base heterojunctions. This bandgap engineering leads to a reduction of hole injection from the base to the emitter, which results in an emitter-injection efficiency γ much closer to 1 compared to a homojunction bipolar transistor. The ratio of the intrinsic carrier concentration between Si and Si_xGe_{1-x} is the well-known Kroemer factor and can be expressed as

$$\frac{n_{i,\text{SiGe}}^2}{n_{i,\text{Si}}^2} = \frac{(N_L N_V)_{\text{SiGe}}}{(N_L N_V)_{\text{Si}}} e^{\frac{\Delta E_g}{kT}} \quad (4)$$

where $(N_L N_V)_{\text{SiGe}}/(N_L N_V)_{\text{Si}}$ is the ratio of the density of states in the conduction and valence band as given in [22]. As the collector and base current directly depend on the intrinsic carrier concentration of the semiconductor material, the current gain β and the emitter-injection efficiency γ are linearly proportional to the Kroemer factor according to

$$\beta = \frac{1}{1/\gamma - 1} = \frac{D_n L_p N_D}{D_p W_B N_A} \frac{n_{i,\text{SiGe}}^2}{n_{i,\text{Si}}^2}. \quad (5)$$

This approach results in an additional degree of freedom, which allows to increase the base doping by orders of magnitude compared to the homojunction bipolar transistor. A typical doping profile of a homojunction [18] and a modern

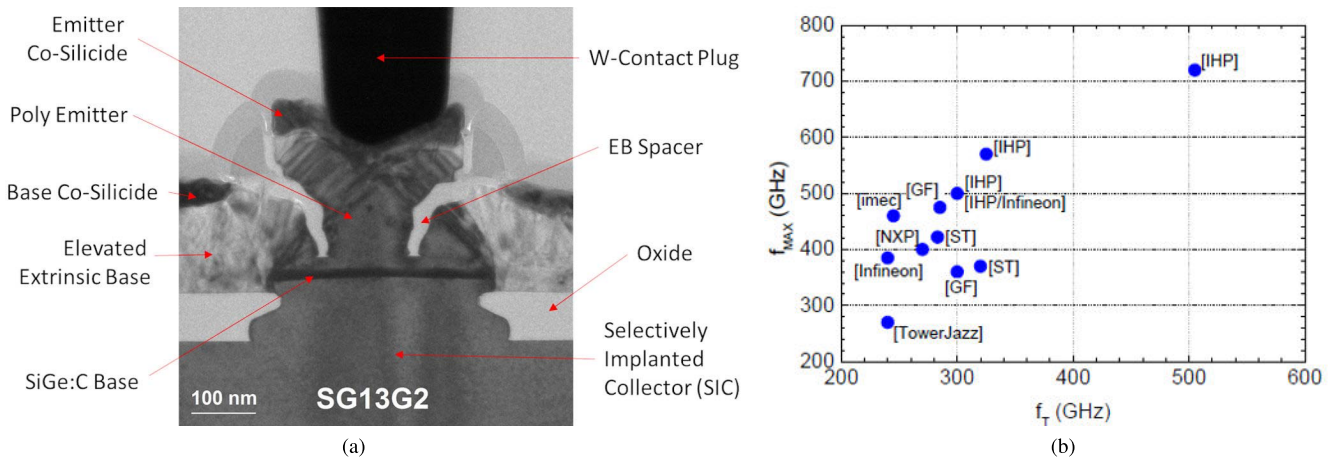


Fig. 2. (a) TEM cross section of a SG13G2 HBT from IHP [26] and (b) peak f_i/f_{max} performance of state-of-the-art SiGe HBT technologies after [27].

SiGe HBT [19] can be seen in Fig. 1. The difference of the emitter–base doping ratio between a homojunction and a heterojunction transistor is clearly visible. An increase of the base doping lowers the base resistance R_B according to (3) and allows to decrease the base width W_B , which results in a lower base transit time τ_B and a higher f_i after (2).

In summary, the introduction of a SiGe emitter–base heterojunction enables an increased base doping $N_{A,SiGe} \gg N_{A,Si}$ and a reduced base width $W_{B,SiGe} \ll W_{B,Si}$, which results in an improved emitter-injection efficiency γ and hence an increased current gain β , reaching values above 1000 for modern SiGe HBT devices [23]. In addition, the transit frequency f_i is increased and the base resistance R_B is reduced. Elevating the base doping additionally reduces the base-width modulation, which increases the early voltage V_A . Altogether, the introduction of the SiGe heterojunction results in an RF and millimeter-wave device with superior electrical properties. As a further improvement of the SiGe HBT, a graded heterojunction with increased germanium fraction toward the collector results in an additional electrical drift field within the base as illustrated in [24] and [25]. This leads to a further reduction of the transit time τ_B through the base and an increase in the speed of the HBT device.

B. Modern SiGe BiCMOS Technologies

Compared to MOS devices, which are characterized by a lateral current flow in a majority carrier inversion layer at the surface of the semiconductor, state-of-the-art bipolar transistors exhibit a current flow vertical to the substrate surface using a series of stacked layers of doped silicon [25]. The vertical semiconductor layers of modern bipolar transistors are realized by doping the silicon bulk material via ion implantation to form the highly doped subcollector, the buried layer, and the collector, while the thin base layer, which is in the range of 10 nm in modern SiGe devices [23], is grown by nonselective or selective SiGe epitaxy and *in situ* doping.

Fig. 2 shows a transmission electron microscopy (TEM) picture of the cross section of a state-of-the-art SG13G2 HBT from IHP [26]. The vertical arrangement of the HBT and the thin base layer of the device are easily identifiable.

Due to the vertical setup within the bulk material and the very well controlled thin base layer, bipolar transistors exhibit a very low defect density leading to $1/f$ noise corner frequencies that are several orders of magnitude lower than in modern CMOS devices. The thin base layer allows for reduced base transit times τ_B that lead to transit frequencies f_i surpassing those of highly scaled CMOS devices. In addition, modern SiGe HBTs offer breakdown voltages BV_{CE0} in the order of 1.4–1.6 V [28], significantly exceeding typical breakdown voltages of modern CMOS devices, which makes HBTs also preferable for medium-power RF and millimeter-wave applications as described in the following.

The large transconductance g_m of today's SiGe bipolar transistors of more than 200 mS/ μm^2 for BiCMOS processes in production and up to 600 mS/ μm^2 for research devices [28] in combination with the high f_i/f_{max} of 320 GHz/370 GHz, e.g., offered by the current 55-nm BiCMOS process from STMicroelectronics [29], allows to bias the device at low collector currents while still offering competitive RF performance, which makes SiGe HBTs also attractive for low-power and battery-operated RF and millimeter-wave applications. Altogether, modern SiGe HBTs exceed the RF performance of highly scaled CMOS devices for millimeter-wave and even THz applications, especially when comparing bipolar and CMOS devices directly and taking the impact of interconnect wiring into consideration.

SiGe HBTs are typically combined with CMOS devices in the form of BiCMOS processes, which are offered by various vendors including IHP [26], ST [29], Tower Semiconductor [30], or Globalfoundries [31]. As a consequence, complex RF and millimeter-wave systems, such as transceivers for communication and radar systems up into the THz range, can be realized, as outlined in Sections III and IV. Modern III–V devices, such as InP HBTs or GaAs HEMTs, still show some advantages, especially regarding the breakdown voltage

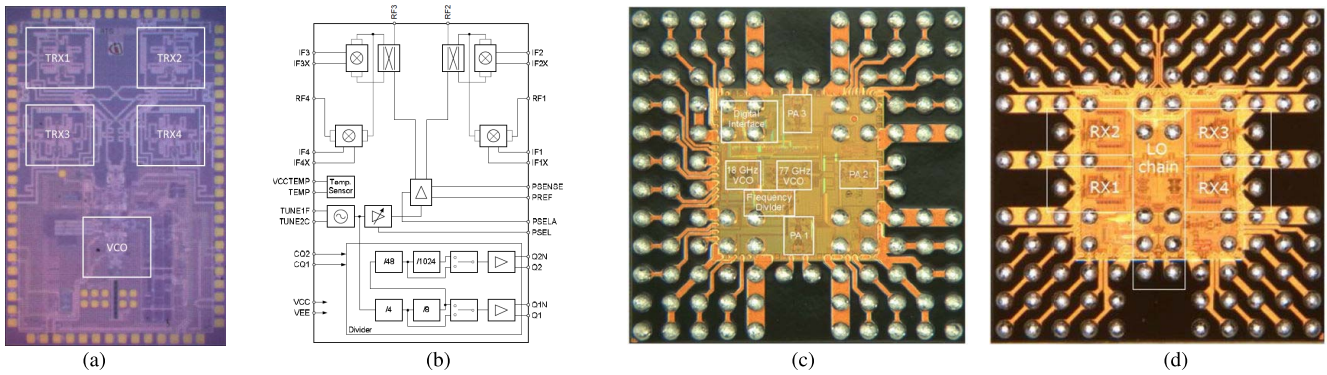


Fig. 3. (a) Photograph and (b) block diagram of the first commercial 77-GHz transceiver [34]. (c) eWLB-packaged 77-GHz transmitter [35] and (d) receiver [36].

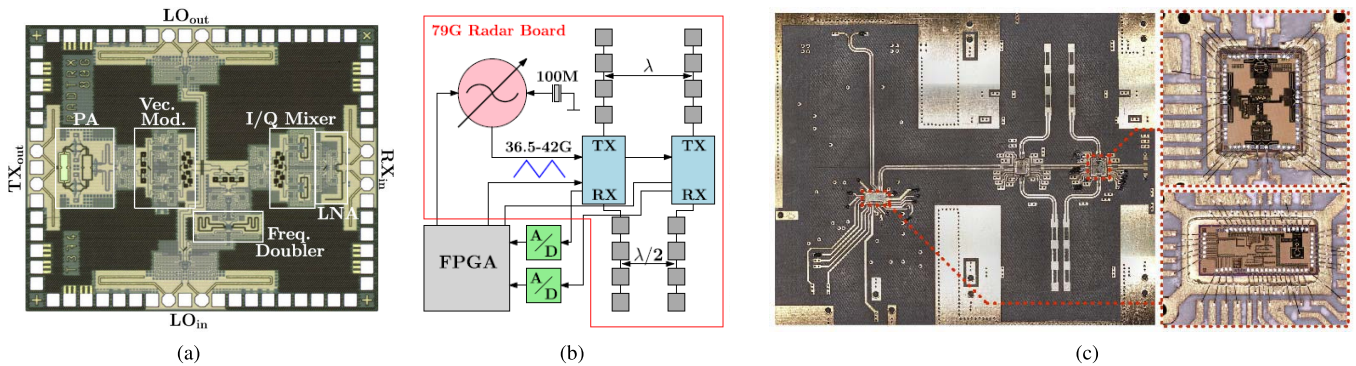


Fig. 4. (a) Chip photograph of a scalable 77-GHz radar transceiver. (b) System concept and (c) demonstrator board of a two-channel FMCW radar system [37].

due to the larger bandgap of the semiconductor materials, but these devices come at the cost of less mature manufacturing processes and severely limited circuit complexity under the constraint of a reasonable process yield. An overview of the current performance of SiGe HBT devices and the status of InP/ GaAsb HBTs is provided in [27] and [32]. Chevalier *et al.* [27, Fig. 2(b)] have shown the f_t and f_{max} performance of various state-of-the-art SiGe HBT/BiCMOS processes. Current development aims to integrate high-performance SiGe HBT devices [28] into a full 130-nm BiCMOS flow. As reported in [33], HBT f_t/f_{max} values of 470/610 GHz have been achieved within a full BiCMOS environment opening new applications for SiGe BiCMOS in the THz frequency range.

III. RADAR TRANSCEIVERS

A. Automotive Radar Transceivers

Automotive radar at 77 GHz has made its way to become the first large-scale commercial millimeter-wave application of SiGe bipolar or BiCMOS technology [38]. An important milestone for the feasibility of SiGe to replace the existing GaAs multichip solutions was the proof of the capability of this technology to provide sufficient output power around 77 GHz. This proof was provided by Li and Rein [39] and Li *et al.* [40] at the beginning of this century and has sparked a massive amount of research interest in the field.

As a consequence, investigations on the improvement of voltage-controlled oscillator (VCO) phase noise [41] and tuning range [42] have been conducted. Furthermore, power amplification techniques were presented [43]–[46] that could provide up to +18 dBm of output power at a peak power added efficiency (PAE) of 9% [45]. In the beginning, mainly dedicated transmitter and receiver components and overall chipsets [47] based on such building blocks were presented. For a variety of reasons, such as lowered assembly cost and improved RF interfacing, the inevitable trend for higher integration levels has led to the realization of highly or fully integrated transceivers [48]. The first complex fully integrated transceiver was published in 2006 [49], [50], followed by the first commercial product in 2008 [34], shown in Fig. 3(a) and (b), and multiple other works [51]–[53]. The first transceivers have been assembled on the RF printed circuit board (PCB) by means of wire bonding with the chip located inside a cavity. As a next step, to improve the reliability and enable standard assembly processes for the system manufacturers, fan-out wafer-level packaging (FOWLP) technologies, also known as embedded wafer-level packaging (eWLB), have been introduced. These technologies, previously used in wireless ICs with high pin count, have been advanced to support low-loss millimeter-wave signaling and interfacing [54]. Fig. 3(c) and (d) shows such realizations for a TX [35] and an RX [36]. Other packaging variants are described in [55] and [56].

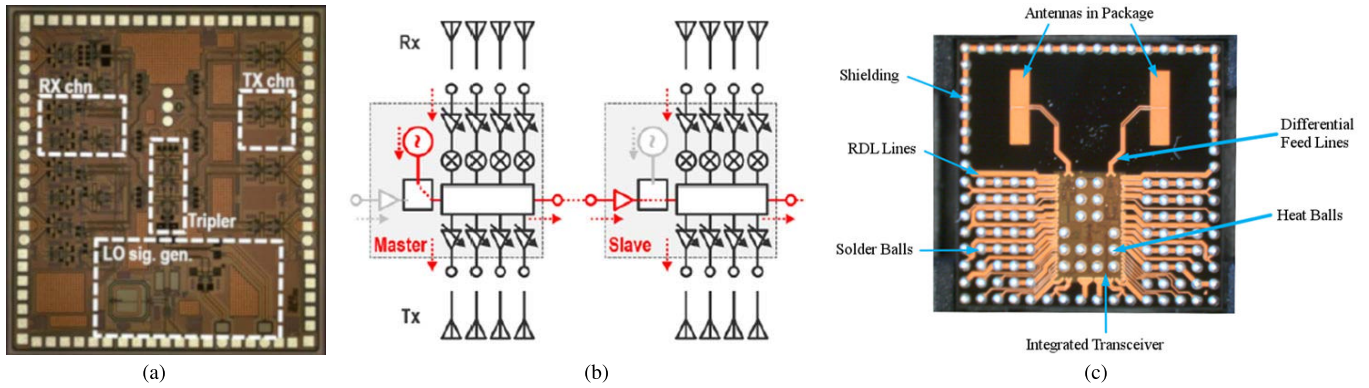


Fig. 5. (a) Chip photograph and (b) cascading concept of a 4TX/4RX 60-GHz transceiver [65]. (c) Single-channel radar transceiver in eWLB package [66].

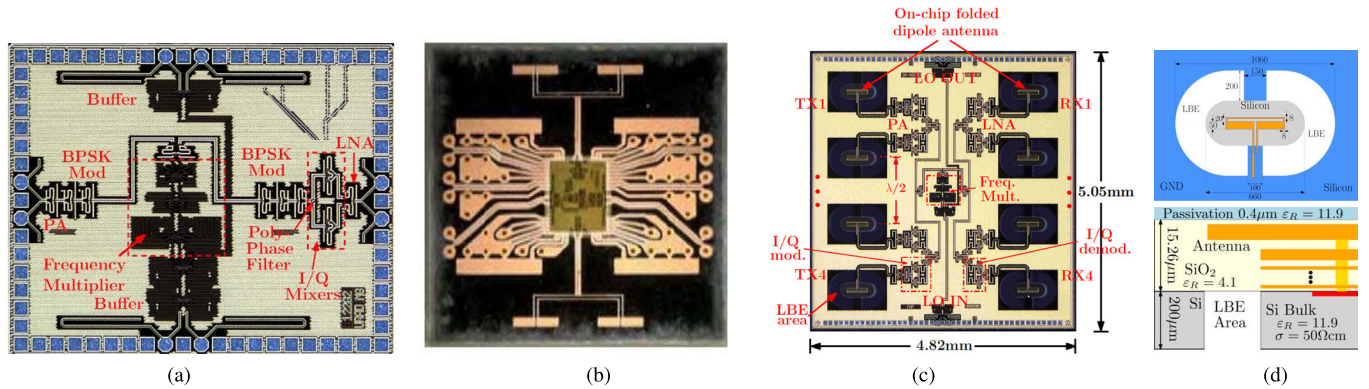


Fig. 6. (a) Photographs of a cascadable 120-GHz transceiver [67], (b) integrated in an FOWLP [68], and (c) 4TX/4RX SoC with on-chip antennas [69]. (d) Illustration of the topside view and cross section of the integrated antennas.

Radar sensors with multiple channels allow for an angular resolving of the illuminated scene and the directive improvement of the signal-to-noise ratio. Two different concepts have been followed here. The first approach is a digital multiple-input–multiple-output (MIMO) architecture [57] that allows a flexible combination of the channels in the digital domain and various operating modes, including pseudorandom sequences [58], [59]. The second is analog beamforming or phased array in the transmitter and receiver [60]–[62], which allows for a better suppression of interferers and reduced signal processing. A practical approach for the combination of multiple transceiver chips to realize complex MIMO systems with many channels is the cascading of ICs in a so-called daisy chain, first proposed by Wagner *et al.* [63], [64]. This technique enables the manufacturing of identical chips of smaller size and hence higher yield at lower cost but puts additional emphasis on the assembly process. Using this principle, a scalable radar platform based on single-channel transceiver circuits has been presented in [37] and is shown in Fig. 4.

B. Industrial and Consumer Radar Transceivers

The availability of integrated VCOs in SiGe technology with a wide tuning range of up to 33% [70] has also led to the realization of radar systems around 77 GHz for nonautomotive applications, such as tank-level sensing, that can operate at much higher bandwidth beyond the 76–81 GHz window. Here,

an ultrabroadband transmitter [71] has been used to realize a frequency-modulated continuous-wave (FMCW) radar with a bandwidth of 25 GHz [72]. Apart from that, several W-band realizations around 94 GHz have been reported [73]–[78]. These include multichannel MIMO realizations [73] as well as phased arrays [75]–[77].

The limited usability of the automotive band and the 94-GHz band, however, favors the use of industrial, scientific, and medical (ISM) bands around 60 and 120 GHz [79]. Especially, the regulation of the 60-GHz band has been relaxed to allow for a use of a widened spectrum of up to 9 GHz. As a result, a number of groups have targeted the demonstration of 60-GHz radar components [80]. Advanced efforts range from single monostatic transceivers [81], [82] to scalable bistatic realizations [67] that contain up to eight channels per IC [65]. Fig. 5(a) shows the die photograph of such a 4TX/4RX integrated radar transceiver in SiGe technology. It features a master/slave concept, where ICs can be configured with an local oscillator (LO) source or cascaded in a daisy-chained slave mode after Fig. 5(b). The aspect of packaging is of similar importance in the 60-GHz band [83]. Here, the aforementioned FOWLP or eWLB approach has been applied in a similar fashion. In addition, the redistribution layer of the package has been used to integrate the antennas into the package [66], [68], [84]. An example of a bistatic 60-GHz industrial radar transceiver with antennas in an eWLB package is shown in Fig. 5(c).

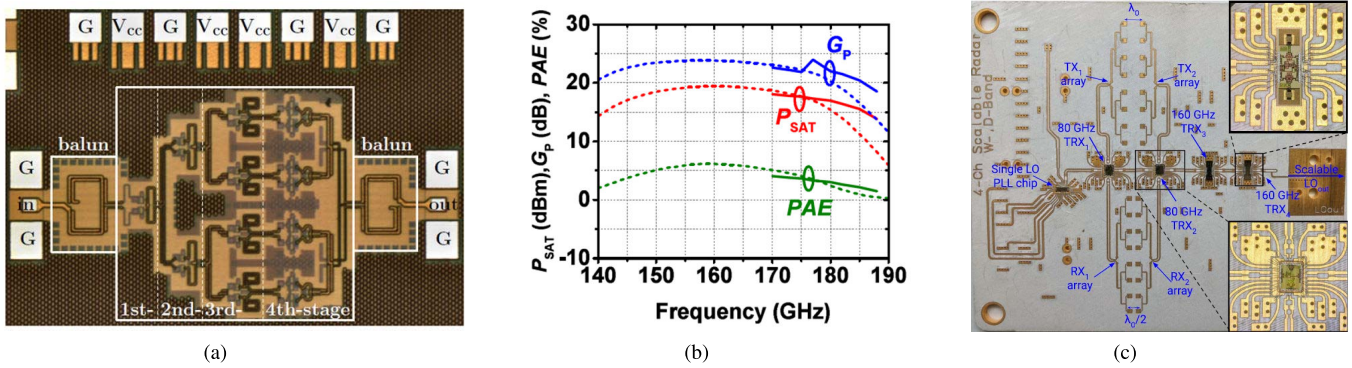


Fig. 7. (a) Chip photograph and (b) measurement results of a D -band power amplifier [93]. (c) Multimode W -/ D -band MIMO radar demonstrator [94].

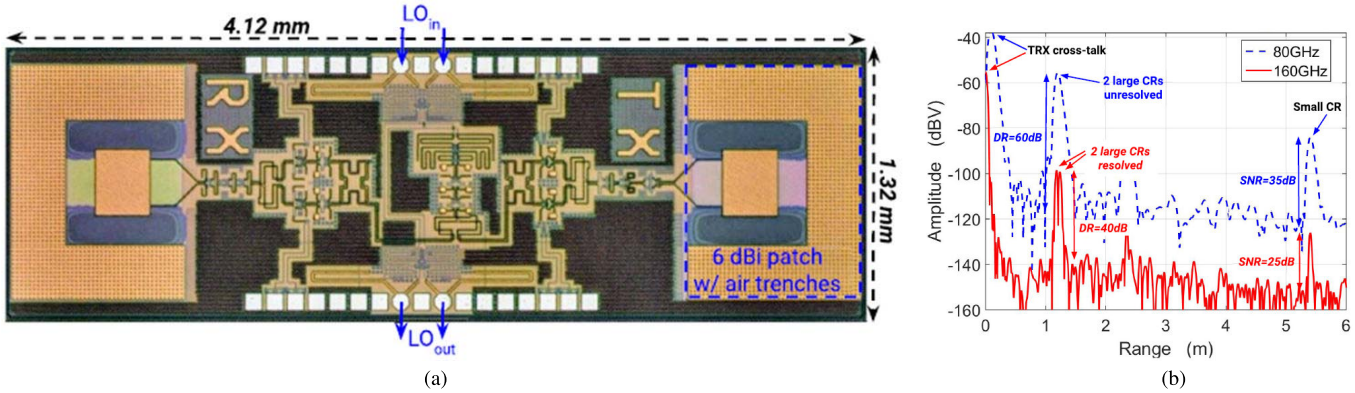


Fig. 8. (a) Die photograph of a bistatic 160-GHz radar transceiver with integrated antennas and (b) ranging results of the 80-/160-GHz multimode radar [94].

The second ISM band located around 120 GHz also received a lot of attention. Here, it could be shown that SiGe is capable of generating sufficient output powers of over +20 dBm [85], [86]. Radar transceivers operating at 120 GHz can still be assembled in a cavity with external antennas on a high-frequency PCB [67], [87], [88]. This approach involves increased losses and bandwidth limitations at the antenna interface, but in return allows for a large aperture. For short-range applications, however, a system-in-package (SiP) approach has been followed [68], [89], [90]. As an example, Fig. 6(a) shows a scalable 120-GHz radar transceiver [67] that has been packaged into an FOWLP, shown in Fig. 6(b), to realize a highly integrated bistatic radar SiP with integrated antennas and low-loss interface [68]. In an even more extreme integration step, the 120-GHz antennas can even be integrated on the silicon chip itself [91]. This provides the least interface limitation, but the bandwidth and efficiency are typically limited by the realizable geometries in the IC metal stack and the losses in the silicon substrate. These losses can be reduced through local backside etching (LBE) [92], which ultimately enables complex systems on chip (SoCs), such as the scalable 4TX/4RX 120-GHz radar transceiver shown in Fig. 6(c) [69].

C. D -Band Radar Transceivers

The D -band spectrum of 110–170 GHz contains several frequency bands for sensing applications that provide significantly more available regulated bandwidth than the

forementioned 120-GHz ISM band. In this frequency range, a number of approaches for signal generation have been published during the last years. They range from frequency multipliers [95] to power amplifiers [93], [96], [97]. Fig. 7(a) shows a chip photograph of a four-way power amplifier that achieves output powers as high as +18 dBm with PAEs around 4% at the upper end of the D -band [93], as shown in Fig. 7(b). The circuit achieves a maximum gain of 30 dB with a 1-dB compression point above +15 dBm. These results prove the feasibility of SiGe technology for radar applications in the D -band and even beyond.

A number of fully integrated radar transceivers have been realized in the D -band. For example, an integrated four-channel transceiver operating at 140 GHz has been introduced in 2012 [98]. Early works on 160-GHz transceivers even date back as far as 2008 [99]. Later, a standalone radar transmitter and receiver chipset at 160 GHz [100] has been presented, where the antennas have been integrated into an eWLB package. Consequently, also 160-GHz radar transceivers in SiGe featuring integrated antenna elements [101] and related MIMO radar systems [102] have been proposed. All these works suffer from a low output power and limited bandwidth of around 15 GHz. This issue has been targeted by other works that seek to cover most of the D -band such as 122–170 GHz [103] and a 104–161-GHz TX/RX chipset [104], where the latter relies on integrated on-chip antennas. However, both examples still only feature low transmitter output powers.

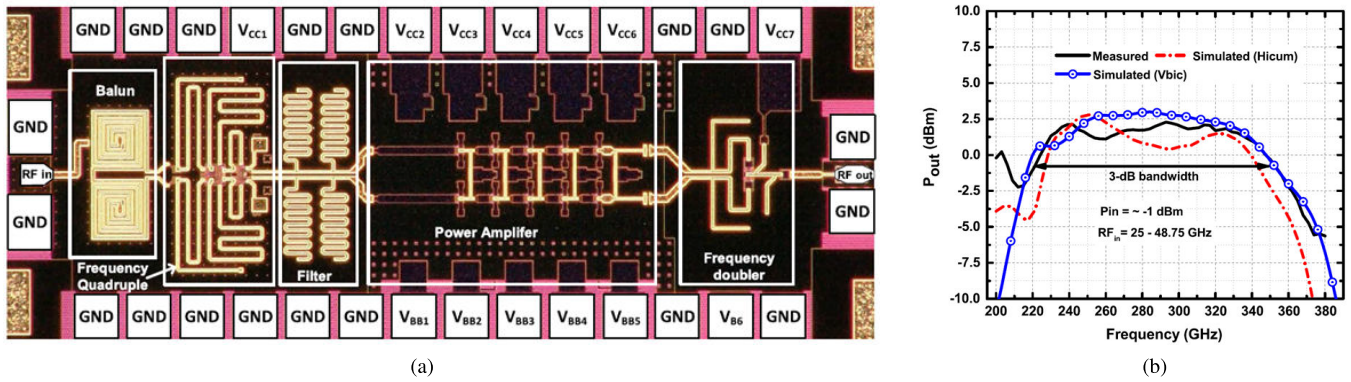


Fig. 9. (a) Chip photograph of a 220–350-GHz frequency multiplier with indicated building blocks and (b) corresponding output power measurement results [105].

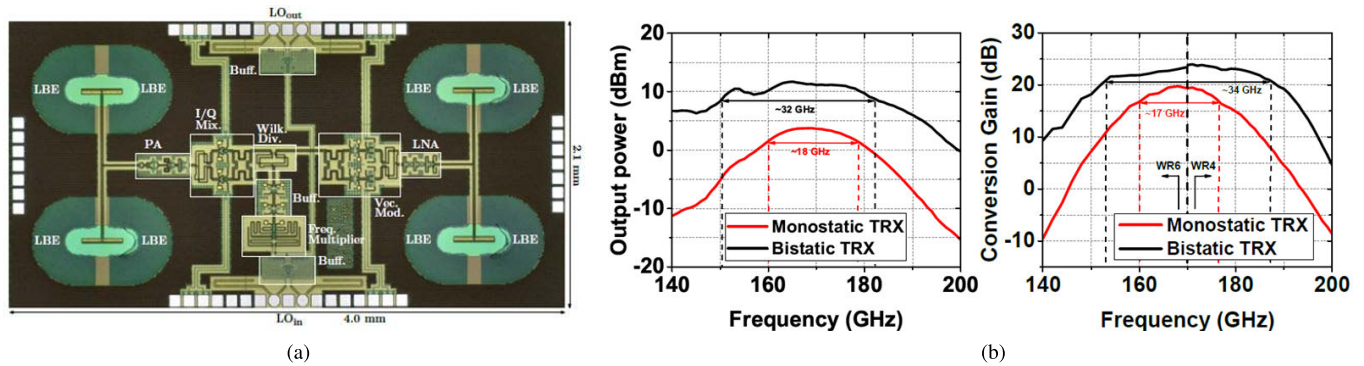


Fig. 10. (a) Chip photograph of a bistatic *G*-band radar transceiver with integrated antennas and (b) measurement results of the TX and RX parameters [106].

Fig. 7(c) shows a recent example of a multimode radar system capable of simultaneously operating in the 80- and 160-GHz band [94]. In the photograph of the PCB, one can see two 80-GHz transceivers connected to an onboard large aperture antenna array for an improved range performance. In addition, the radar features two 160-GHz transceivers on the right, which are directly daisy-chained to the previous 80-GHz elements. These ICs feature integrated antennas with an increased bandwidth. The detailed chip photograph of the highly integrated 160-GHz transceiver is shown in Fig. 8(a). One can clearly identify the TX and RX patch antennas with accompanying air trenches on the left and the right of the chip area. The circuit consumes 1 W, occupies an area of 5.4 mm², and features a transmitter output power of +13 dBm. Due to this high output power, a bistatic configuration with dedicated antennas was chosen to increase the isolation between TX and RX. The IC further contains a frequency quadrupler to seamlessly fit into the scalable channel concept. Due to this additional multiplication by two, compared to the 80-GHz transceiver, the multimode radar system is capable of resolving more closely located targets, as shown in Fig. 8(b). Here, two corner reflectors (CRs) at 1.2 m in close distance proximity can be distinguished with the 160-GHz transceivers (red line) opposed to the original 80 GHz (blue dashed line).

D. Toward THz Radar Transceivers

The aforementioned four-way power amplifier in [93] also extends beyond the *D*-band and provides output powers

above +10 dBm up until around 200 GHz. Higher operating frequencies are typically achieved by means of frequency multiplication [107], [108]. Here, a frequency octupler in SiGe with an output power above 0 dBm and a record 3-dB bandwidth even exceeding the waveguide *J*-band (220–325 GHz) has recently been shown [105]. The chip micrograph of said octupler is shown in Fig. 9(a). It is comprised of a frequency quadrupler with spur filtering at the output, followed by a broadband *D*-band power amplifier that drives a frequency doubler. The output power and associated bandwidth for an input power of around -1 dBm are shown in Fig. 9(b). The circuit can deliver typical LO driving powers for mixers of 0 dBm up to a frequency of 350 GHz. Other methods of signal generation include the realization of integrated VCOs at such high frequencies [109]–[111]. Here, push–push oscillators operating at half the single-ended output frequency are favored. Oscillators provide the advantage of a higher dc-to-RF efficiency but generally suffer from a limited bandwidth, especially at such high frequencies. Nevertheless, tuning ranges around 10% in combination with output powers exceeding 0 dBm could be realized in the referenced papers. Signal sources based on coupled arrays of oscillators have been the subject of many recent studies, not only in CMOS but also in SiGe technology [112], [113]. Here, the idea is to increase the radiated output power through the integration of many oscillators with dedicated antennas and subsequent free-space power combining yielding up to +3-dBm radiated power. A corresponding TX/RX chipset with a subharmonic RX for imaging applications has been presented in [114]. Such

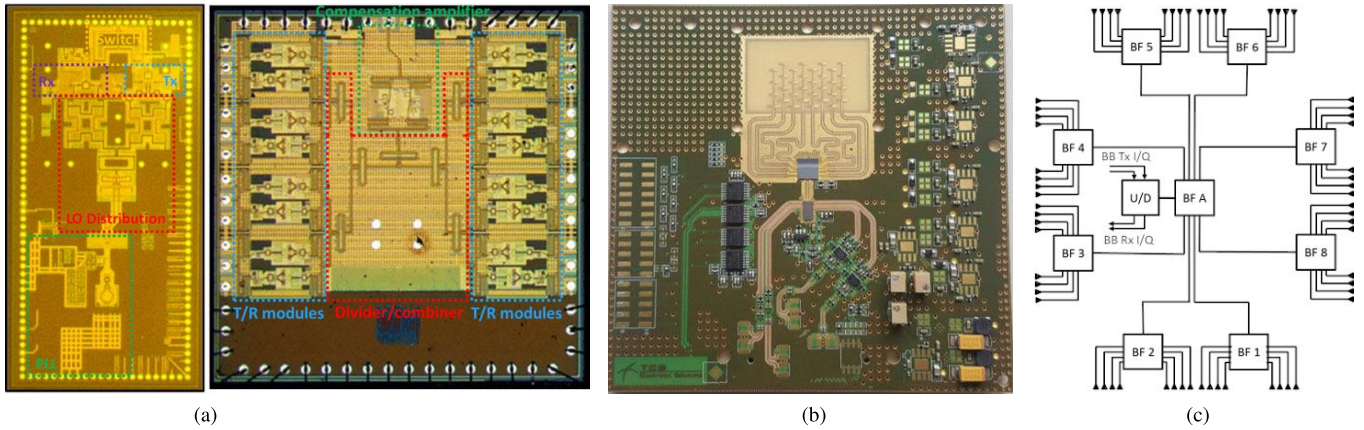


Fig. 11. Die photographs of (a) 60-GHz up/down-converter and eight-channel transceiver, (b) PCB mounting, and (c) possible backhaul array configuration [121].

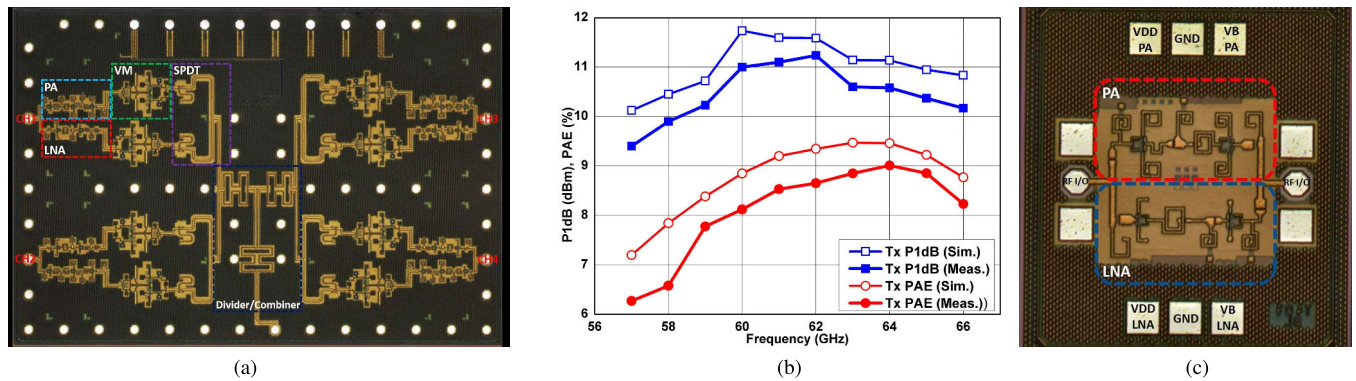


Fig. 12. (a) Chip photograph of a 60-GHz four-channel T/R module with switchless antenna port [122] and (b) measurement plus (c) photograph of the PALNA [123].

subharmonic RXs are an alternative approach to push-push oscillators or frequency multipliers and allow for the proliferation of mixers with an LO signal at half the desired operating frequency. They have first been explored around 220 and 320 GHz in [115].

First implementations of fully integrated radar transceiver front ends around 170-GHz featured a bandwidth of 27.5 GHz and radiated powers of -1 dBm [116]. The latest results in this frequency range are presented in Fig. 10. Here, Kucharski *et al.* [106] demonstrated an integrated bistatic radar transceiver, shown in Fig. 10(a) with $+13$ -dBm output power and 3-dB bandwidths above 30 GHz. Other works have focused on the 240-GHz range with notable results such as equivalent isotropically radiated power (EIRP) values in combination with integrated antennas of 0 to $+3$ dBm and bandwidths of up to 60 GHz [117], [118]. The first integrated THz radar transceiver front end above 300 GHz in SiGe was proposed in [119]. It operates at 380 GHz, relying on a frequency quadrupler in the transmit path and a doubler plus subharmonic mixer in the RX. The circuit also features integrated antennas, but due to an EIRP below -10 dBm and an RX noise figure (NF) above 35 dB, operation was limited to the centimeter range. Nevertheless, recent results suggest that radar transceivers with 0-dBm radiated output power can be realized around 340 GHz [120].

IV. COMMUNICATION TRANSCEIVERS

A. 60-GHz Communication Transceivers

The development of integrated transceiver components in SiGe for 60-GHz wireless personal area networks marks the beginning of the still ongoing exploration of silicon millimeter-wave technologies for wireless communication applications. This pioneering work has been carried out at IBM at the beginning of this millennium [124]. As a result, a 60-GHz transmit/receive (TX/RX) chipset has been presented in 2006 [125]. The concept was based on an IQ-mixer architecture with an LO frequency tripler to enable the combination with a 20-GHz phase-locked loop (PLL). In this work, a TX saturated output power of $+15$ to $+17$ dBm and a 1-dB compression point of $+10$ to $+12$ dBm was achieved, while the RX featured an NF of 6 dB. This chipset was combined with a planar antenna and a wireless link at a speed of 630 Mb/s over a distance of 10 m was demonstrated. Subsequent works proved the capability of SiGe to enable output powers as high as $+23$ dBm [126]. Also, an approach for a full integration of a 60-GHz chipset into a cost-effective plastic package, including the TX and RX antennas, was presented [127]. In the following, the focus was set on the integration of complex 16-channel transmitters [128] and corresponding receivers [129] to enable

TABLE I
OVERVIEW OF CURRENT U.S. AND EU FREQUENCY REGULATION FOR INDOOR AND FIXED OUTDOOR SERVICES [133]

Type	Band	Region	Frequency Range	max. Bandwidth	max. TX Power	max. EIRP	Antenna Gain
Indoor	60GHz	US	57-64 GHz	7 GHz	+27 dBm	43 dBm	
		EU	57-66 GHz	9 GHz		40 dBm	
Fixed Outdoor	60GHz	US	57-64 GHz	7 GHz	+27 dBm	85 dBm	51 dBi nom.
		EU	57-66 GHz	9 GHz	+10 dBm	55 dBm	30-45 dBi
			64-66 GHz	2 GHz	+35 dBm	85 dBm	30-50 dBi
	70/80 GHz	US	71-76 GHz / 81-86 GHz	5 GHz (each)	+35 dBm	85 dBm	43-50 dBi
		EU					38-55 dBi
90 GHz	US	92-95 GHz	2 GHz (92-94 GHz) 0.9 GHz (94.1-95 GHz)	+35 dBm	85 dBm	43-50 dBi	

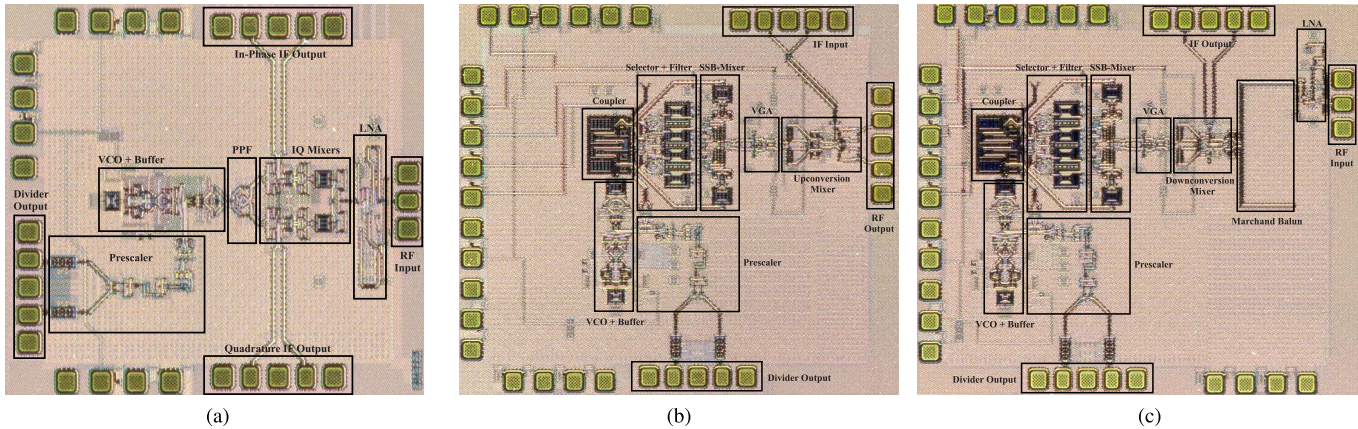


Fig. 13. Die photographs of (a) 70–90-GHz IQ RX [134] and (b) heterodyne 50–100-GHz transmitter and (c) receiver chipset [135] for backhaul.

electronic beamforming with spatial power combining, where each TX path features a P1dB of +9 to +13 dBm, and a packaged TX with an EIRP of +40 dBm was realized. The receiver supported a 5-Gb/s data transmission experiment using 16-QAM [orthogonal frequency-division multiplexing (OFDM)] modulation. Finally, an 802.11ad/WiGig-compliant transceiver in SiGe in an organic ball-grid array (BGA) package with in-package antennas was presented in [130]. The largest EIRP of +45 dBm, so far, has been demonstrated using a wafer-scale approach, where 256 elements were combined in a massive single wafer array [131].

The latest approaches rely on a scalable concept based on individual phased-array transceiver (TRX) with a limited amount of channels per IC. These are typically realized via multiple bidirectional transmit/receive (T/R) modules [121]–[123], [132]. Here, EIRPs around +40 dBm have been achieved and used to demonstrate data transmission of 1–4 Gb/s over hundreds of meters [132]. An example for one of the first realizations of a bidirectional beamforming TRX is shown in Fig. 11 [121]. The chipset is comprised of an upconverter/downconverter IC and an eight-channel beamformer shown in Fig. 11(a). The chips have been mounted on a board according to Fig. 11(b) that can be varied in size through a scalable concept after Fig. 11(c). The integrated beamformer has recently been enhanced through the implementation of switchless T/R modules after Fig. 12(a) [122]. A chip photograph of a single bidirectional switchless T/R stage, also known as a PALNA, is shown in Fig. 12(c) [123]. This concept

removes the lossy switches at the antenna ports and allows an increased TX P1dB of +10 dBm [see Fig. 12(b)].

B. E-/W-Band Communication Transceivers

Besides the 60-GHz band with main applications in personal WiFi networks, other applications related to point-to-point connections, such as wireless backhaul/infrastructure, have been considered for SiGe technology. Table I shows an overview about the U.S. and EU regulations for indoor and fixed outdoor services [133]. The EIRP needs to be reduced by 2 dB for every 1-dB antenna gain less than the given value. One can observe that significant bandwidths and allowed EIRPs are possible for fixed point-to-point links in the bands above the 60-GHz range. The most attractive are the E-band (70–90 GHz) communication windows located below (71–76 GHz) and above (81–86 GHz) the automotive radar band with two times 5 GHz of available bandwidth. Here, +27-dBm saturated output power has been achieved using a 16-way amplification concept [136]. Beyond that, a recent PA design could even demonstrate a P1dB of +20 dBm with PAEs around 20% [137].

Naturally, also complete TX and RX integrations have been the subject of research over the past years. In 2010, a quadrature (IQ) transceiver in SiGe technology featuring +9-dBm output power and NF of 7 dB for the lower 70–80-GHz band was presented [138]. Fig. 13(a) shows the die photograph of a multiband IQ RX that is capable of

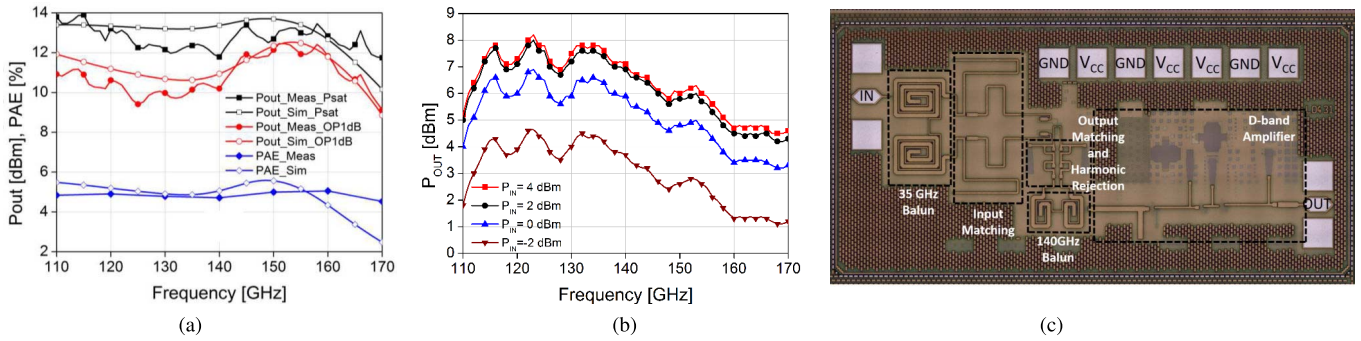


Fig. 14. Individual measurement results of (a) full *D*-band power amplifier [149] and results of (b) frequency multiplier including (c) chip photograph [150].

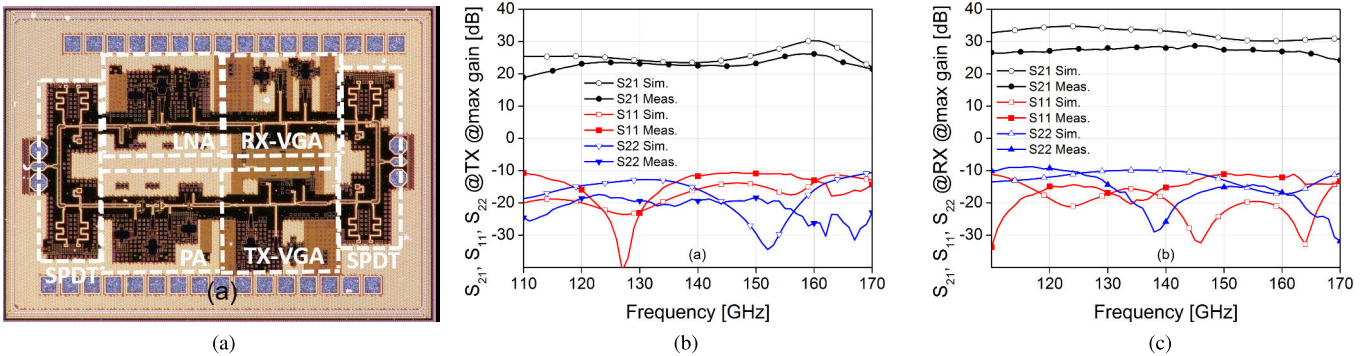


Fig. 15. (a) Full *D*-band transmit/receive module for potential 6G communication with (b) transmitter and (c) receiver S-parameter measurements [151].

covering both bands from 70 to 90 GHz [134]. Finally, a high-performance full *E*-band TX/RX chipset has been published in [139]. It relies on a heterodyne architecture and features a saturated transmit power and 1-dB compression point of around +20 and +17 dBm, respectively. A particularly elegant system concept for bidirectional phased arrays in the *E*-band, based on injection-locked phase-shifting, has also been presented [140]–[142]. Here, the detuning of the natural oscillation frequency of injection-locked oscillators is used to realize an LO phase shifting architecture. Due to the limitation to below $\pm 90^\circ$, frequency quadruplers were used, which also multiplies the phase range by the same factor.

The remaining *W*-band above 90 GHz has also been targeted for communication applications. Here, a wafer-scale concept was applied again to a 16-element transmitter at the upper edge of the band (110 GHz) [143]. Due to the high carrier frequency, on-chip antennas have been used and an EIRP of +25 dBm was achieved. In [135], the feasibility of ultrabroadband single-channel heterodyne front ends that can cover all wireless communication bands in Table I has been proved. The chip photograph of the 50–100 GHz transmitter and receiver is shown in Fig. 13(b) and (c). Around the same time, 94-GHz phased arrays started to appear in the literature. For example, IBM published a 16-element dual-polarization transceiver based on bidirectional T/R modules with an output 1 dB-compression point of 0 dBm [144]. Later, the same group also presented a 16-element dual-polarization TX/RX chipset with an OP1dB of +4 dBm and saturated power of +8 dBm [145]. Excellent works on broadband 70–100-GHz phased-array communication transceivers have also been

performed by Bell Labs. Here, a four-element TX/RX chipset with +5-dBm saturated output power [146] and related chipsets with up to 16 TX or RX elements per IC achieved a peak EIRP of +34 dBm with data rates of 30 Gb/s at 1 m [147] and even +52 dBm with 10 Gb/s at 250 m when tiled into a 256-TX PCB array [148].

C. *D*-Band Communication Transceivers

First efforts toward *D*-band communication systems based on IQ transmit/receive chipsets date back until the beginning of the last decade [152], [153]. These early works were still limited in terms of bandwidth to below 20 GHz but could already show saturated output powers as high as +10 dBm, albeit with a significantly lower output-referred compression point (P1dB) around 0 dBm. However, following encouraging examples in indium-phosphide technology [154], in recent years, the state-of-the-art has been pushed significantly with a number of works that target full coverage of the *D*-band from 110 to 170 GHz [149]–[151], [155]. Fig. 14(a) shows the measurement results of a three-stage cascode stagger-tuned *D*-band power amplifier [149]. By means of exploiting a number of bandwidth enhancement techniques, the design achieves saturated output powers around +13 dBm over the complete 110–170-GHz band. Even more importantly, an output-referred 1-dB compression point of +9 to +12 dBm has been achieved. Furthermore, a broadband 110–170 GHz frequency multiplier chain as an LO source for an accompanying upconverter/downconverter with a multiplication factor of four in SiGe technology has recently been realized [150].

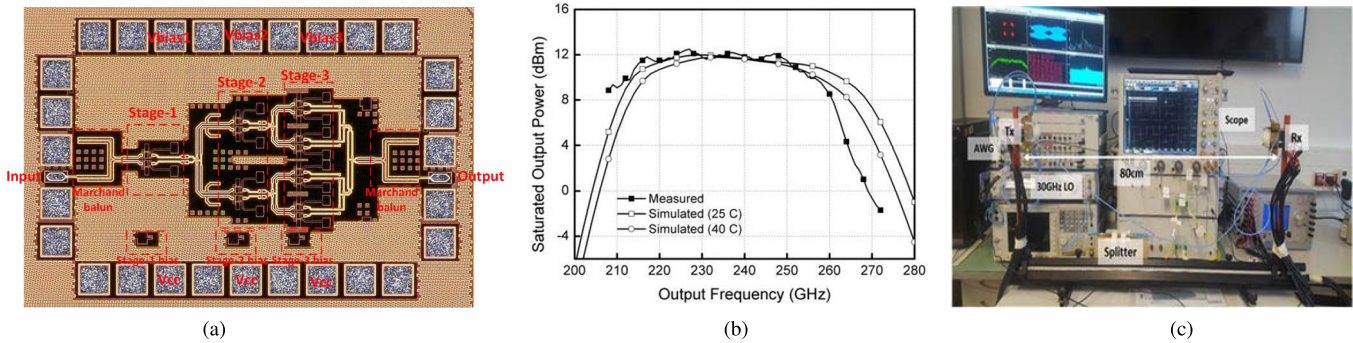


Fig. 16. (a) Four-way power amplifier, (b) measured output power before deembedding [158], [159], and (c) measurement setup for wireless link [160].

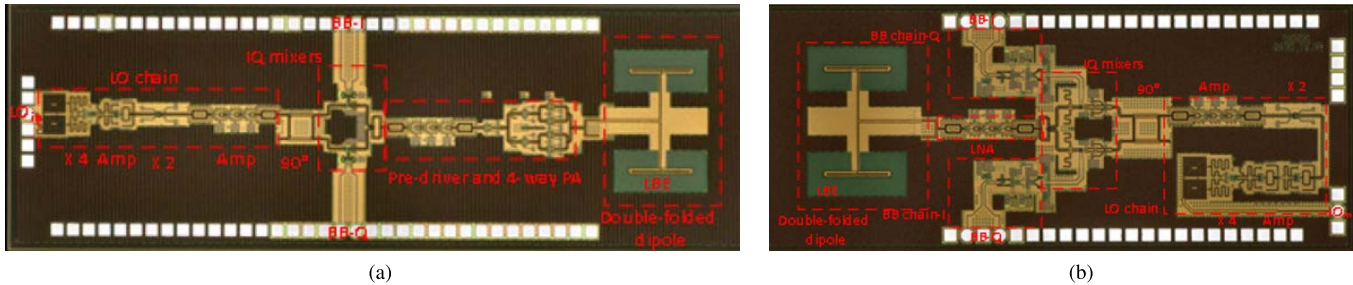


Fig. 17. Chip photos of (a) 100-Gb/s data rate transmitter and (b) receiver chipset, operating at 240 GHz for wireless short-range communication [160].

Selected measurement results are shown in Fig. 14(b). The circuit shows an output power of around +5 to +8 dBm over the complete 110–170-GHz band and can be used to drive a dedicated I/Q modulator or demodulator with two mixer cells. The multiplier chip photograph is shown in Fig. 14(c). It is comprised of a Gilbert cell-based quadrupler with second-harmonic rejection at the output plus a subsequent broadband *D*-band amplifier.

Recently, the first step toward higher system integration has been undertaken. In [155], a TX and RX phased-array amplifier chipset for a radio-on-glass communication module has been presented. Both ICs feature a digitally controlled vector-added phase shifter and a low-noise amplifier and power amplifier, respectively. The concept achieves an RX NF of 10 dB and a TX 1-dB compression point of +10 dBm and operates over a bandwidth of 130–170 GHz. An even higher RF integration level has been demonstrated in [151]. It introduces a broadband bidirectional transmit–receive (T/R) module in SiGe technology for phased-array applications. The chip photograph of the circuit is shown in Fig. 15(a). The module includes two broadband single-pole double-throw switches with a low insertion loss around 2 dB and high power handling capability of +17 dBm. In the RX mode, an integrated three-stage cascode LNA plus variable-gain amplifier (VGA) provides a peak gain of 28 dB over the entire 110–170-GHz band and a minimum NF of 9 dB. When operated in the TX mode, a three-stage PA in combination with a TX-VGA delivers 22-dB gain at 113–170-GHz bandwidth. Here, a saturated output power close to +10 dBm is reached with a P1dB of +7 dBm. The measured S-parameters of the module in TX and RX modes are shown in Fig. 15(b) and (c), respectively.

Apart from the aforementioned efforts in broadband *D*-band phased-array circuits, an increased effort is also spent on the investigation of digital-to-analog converter (DAC) and analog-to-digital converter (ADC)-less architectures that can still support higher order modulation [156], [157] with the potential to significantly decrease overall power consumption.

D. Toward THz Communication Transceivers

At the THz frontier of 300 GHz, the challenges in the realization of high-speed transceivers in silicon with the capability of functioning over a reasonable distance are manifold. These challenges can be summarized as: very small maximum available gain, low output power, elevated minimum achievable NF, limited transistor modeling, and measurement accuracy. Despite all these difficulties, wireless communication transceivers in SiGe operating in the THz regime beyond 300 GHz have been proposed [161], [162]. However, both approaches are based on a nonfundamental modulation in the transmitter, which limits the data bandwidth and makes them unsuitable for most broadband communication applications due to phase multiplication and amplitude distortion in the subsequent frequency multiplier.

For the above reasons, the frequency range located between 170 and 300 GHz has so far been the main target for short-range wireless transceivers. The key argument is the higher achievable output power. Here, signal sources that rely on frequency multiplication have mainly been used [163]–[165]. All of the mentioned works implement frequency doublers, driven by an amplifier stage, to generate output powers of +6 to +8 dBm in the frequency range from 200 to 260 GHz. Recently, it has also been shown that fundamental signal amplification in this frequency range is

still possible [158], [159], [166]. Fig. 16(a) shows the die photograph of a four-way power amplifier centered around 240 GHz [158]. Its output characteristics before deembedding are shown in Fig. 16(b). Using this concept, the saturated powers of +13 dBm (without balun) and a P1dB of +10 dBm at a 3-dB bandwidth of 200–255 GHz with a gain of 15 dB have been demonstrated [159].

Such favorable characteristics have led to the investigation of fully integrated communication transmitters and receivers in SiGe technology [167]–[171]. Based on these single-element transmitter and receiver chips, high-data-rate links were demonstrated reaching 100 Gb/s [160], [172] for distances ranging to a maximum of 1 m. Fig. 16(c) shows a photograph of an experimental setup of said 100-Gb/s link using 16-QAM data formats around 240 GHz [160]. For distances in the range of a meter, additional focusing elements such as quasi-optical lenses are still required in all presented works. The chip photographs of the employed transmitter and receiver chip are shown in Fig. 17(a) and (b). Both ICs use an identical frequency multiplier chain by eight to convert an external 30-GHz LO signal into the carrier frequency. The chips feature an IQ-modulator and demodulator to support DAC-less QPSK modulation. The RX further includes a 240-GHz low-noise amplifier, whereas the transmitter comprises the aforementioned four-way power amplifier. Finally, both chips include an on-chip double-folded dipole antenna with localized backside etching of the lossy silicon beneath the antennas.

Although these results represent an important milestone as a proof of concept, future THz communication systems have a lot of room for research to emerge as power efficient and yet compact solutions. For example, the high-bandwidth IF interfaces require additional measures to channelize the baseband data streams at the TX and RX sides [171]. Efforts to realize complex communication phased arrays, similar to current *W*- and *D*-band solutions, that allow flexible electronic beam steering without focusing elements in this THz frequency range are under way, but so far have been limited to the demonstration of individual building blocks [173].

V. FUTURE DIRECTIONS

Although CMOS scaling is still a topic for SiGe BiCMOS technologies [29], [31], their CMOS nodes clearly lag behind several generations compared to the state-of-the-art of CMOS-only processes. The main advancement of SiGe BiCMOS process technology focuses on a “More than Moore” approach, targeting the increase of functionality and performance as an orthogonal way to pure “More Moore” CMOS scaling. Currently, three main directions of enhancement of modern BiCMOS processes can be identified: 1) improvement of the high-frequency SiGe HBT performance toward f_i/f_{\max} values in the THz region; 2) monolithic integration of new technology modules such as silicon photonics in an electronic-photonics integrated circuit (EPIC) or neuromorphic devices into the BiCMOS process flow; and 3) heterogeneous integration approaches combining the best of various technologies to achieve a superior overall system performance. Apart

from these monolithic advancements, continuous effort is spent toward seamless design and simulation of multitechnology assemblies to overcome borders in module and system design.

A. THz Performance

Current SiGe BiCMOS processes offer an f_i/f_{\max} of around 300/450 GHz [26], [29], [31]. In principle, this allows the design of SiGe systems even above 300 GHz, but the main shortcoming is the possibility to generate gain and output power at these frequencies. Commonly used approaches use frequency multipliers driven by power amplifiers [105] or implement subharmonic mixers [175]. A more efficient but narrowband approach is the direct combination of a subharmonic oscillator with a doubler or push–push operation [109]. Obtaining more output power is either achieved by a parallel combination of multipliers [176] or free-space power combination of multiple radiating elements [177]. However, such approaches require significant silicon die area. Within the European DOTSEVEN [178] and TARANTO projects [179], the path to true THz operation of SiGe HBTs has been laid. The objective of these projects was to develop a device platform exceeding f_{\max} of 600 GHz to be used in the next generation of Infineon’s 130-/90-nm and STs 55-nm BiCMOS processes, while IHP was pushing f_{\max} toward 700 GHz. As the current state-of-the-art, a SiGe HBT f_i/f_{\max} performance of 505/720 GHz was presented in [28], enabled by an optimized vertical profile, lateral device scaling, a decreased base and emitter resistance via rapid thermal annealing, and a low-temperature backend. When integrated in a 130-nm BiCMOS process environment, f_i/f_{\max} of 470 GHz/610 GHz has been achieved [33]. Both characteristics are shown in Fig. 18(a) and (b). This performance allows true RF power generation in the THz regime without the need for frequency multiplication extensive power combining techniques, opening up new applications for submillimeter-wave sensors and communication systems. Current research indicates that further f_i/f_{\max} performance increases toward 1 THz seem feasible, which would ensure SiGe HBTs a long-term leading position for millimeter-wave and THz circuits.

B. Electronic-Photonic Integration

Photonic links have been a key technology for long-distance and high-speed communications for a long time. Recently, silicon photonics has become a game changer for these applications, fully unfolding its potential if monolithically combined with silicon technology that is capable of providing high-speed electronic devices. Such a monolithic cointegration of electronic and photonic components enables significantly lower interface parasitics and manufacturing costs if compared to hybrid electronic-photonics assemblies. Here, compared to CMOS devices, the availability of SiGe HBTs within an EPIC process offers advantages with respect to a higher f_i/f_{\max} and increased breakdown voltages BV_{CE0} . A monolithic EPIC platform cointegrating silicon photonic devices into a high-performance BiCMOS environment is demonstrated in [174]. It combines optical modulators, broadband photodetectors, and optical waveguides with the performance

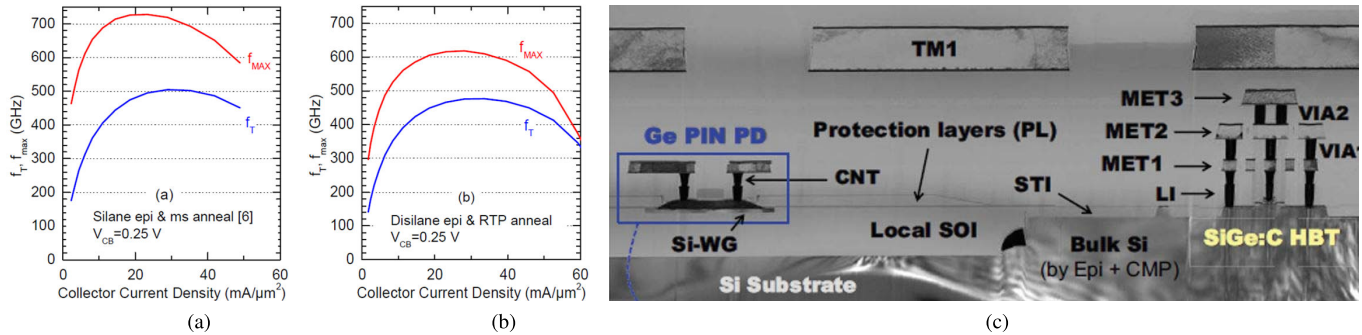


Fig. 18. (a) Standalone SiGe HBT module f_t/f_{max} performance and (b) reduction if integrated into a 130-nm BiCMOS process environment [33]. (c) Cross section of a 250-nm BiCMOS EPIC technology including Ge-photodiodes and waveguides in local SOI and SiGe HBTs in an adjacent Si-bulk region [174].

of a 250-nm BiCMOS technology offering SiGe HBT devices with an f_t/f_{max} of 220/290 GHz. Fig. 18(c) shows a cross section of this EPIC technology, which leverages local silicon-on-insulator (SOI) for the photonic components and selective epitaxial grown bulk silicon for the high-performance electronic components [180]. Beside applications related to high-speed optical communication [181]–[184], EPIC technologies have also successfully been applied for sensor applications [185], [186], showing its great potential. Significant progress has been made recently, pushing the Ge-photodiode bandwidth toward 110 GHz [187], which will enable the use of this technology for next-generation silicon photonic data communication. As the need of Si-photonics-based technologies is constantly growing, an increased number of semiconductor vendors and research organizations offer open access to silicon-based EPIC platforms, which will further boost this technology [174], [188]–[190].

C. Heterogeneous Integration

As discussed in Section V-B, monolithic integration of additional functional modules, such as silicon photonics or neuromorphic devices into a BiCMOS technology, enables significant advantages from the application point of view, such as low parasitics, small form factor, and low manufacturing cost. Still, the monolithic integration of such functional modules in a CMOS-compatible environment without degrading transistor performance is a great challenge. This effort only makes sense for a limited type of functionalities and technologies considering the overall feasibility and economic impact. In particular, when combining different types of semiconductor materials such as silicon and III–V semiconductors, aspects, such as diverging crystal lattice constants leading to stress and dislocations, impose major challenges and even roadblocks that have not been solved successfully.

A key to combine divergent technologies is the approach of heterogeneous integration. Rather than following the classical “More Moore” path of ever increased performance and functionality by further scaling CMOS based SoCs, heterogeneous integration is a “More than Moore” approach, combining different technologies to realize SiPs or systems on modules (SoMs) to boost performance and functionality [193]. Often, the combination of different chip-level technologies is realized either by interposer technologies, often using organic PCB materials, or advanced packaging technologies, such as

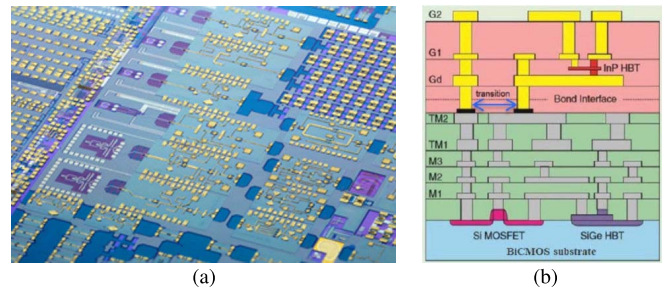


Fig. 19. (a) Wafer photograph [191] and (b) vertical layer stack [192] of the wafer-bonded InP DHBT/SiGe BiCMOS heterogeneous integration technology.

FOWLP [194] that offers superior high-frequency performance at low manufacturing cost. The 3-D stacking of different chips is an attractive alternative utilizing the third dimension, which further reduces the module’s form factor. This in combination with through-silicon vias (TSVs) is one of the heterogeneous enablers, especially when aiming at the THz range [195].

A promising path to increase the performance of next-generation millimeter-wave and THz systems is the combination of SiGe BiCMOS with InP HBTs [192], which can be based on a waferbonding process of SiGe and InP wafers as described in [191]. This combination enables the utilization of the circuit complexity offered by an advanced SiGe BiCMOS process together with an InP HBT f_t/f_{max} of 350/350 GHz and InP HBT breakdown voltages BV_{CE0} in the range of 4 V. Fig. 19(a) shows a photograph of such a combined InP-on-BiCMOS wafer. As the waferbonding of SiGe with InP still shows major disadvantages, such as the large difference in wafer size and yield, the next step toward heterogeneous integration of SiGe with InP will be based on a chiplet approach as described in [196] and [197], which is a special type of flip-chip assembly. The sole combination of InP with pure CMOS, although appealing, potentially leads to low yield when replacing all SiGe transistors with InP and additionally suffers from the f_t/f_{max} limitations of the CMOS metal stack [198].

When designing a heterogeneous integrated system, not only the semiconductor chips but also additional crucial subcomponents such as the interconnects between chips, package, and interposer have to be designed in a codesign manner. In addition, thermal management and thermomechanical aspects have to be considered carefully when bringing together various

material systems. As a result, successful development of heterogeneous integrated systems relies on a complex and seamless design methodology, including 2.5-/3-D electromagnetic (EM), thermal, and thermomechanical FEM design. Significant effort has been spent in the field of heterogeneous design methodology [199], [200], but more work still lies ahead to unleash the full potential of heterogeneously integrated systems.

The integration of a complex phased-array system is of paramount importance for the success of future silicon millimeter-wave and THz solutions. Here, the increasing packing density of tiles with decreasing wavelength requires novel concepts in antenna cointegration and package codesign. A recent comprehensive overview is provided in [201].

D. THz CMOS

CMOS technology is the natural choice for applications that significantly exceed 1 million units per year, due to its unrivaled low-cost mass manufacturing and high integration density. Consequently, CMOS has taken over many of the fields originally owned by SiGe, such as 60-GHz wireless communication [202] and consumer/automotive radar in the 60- and 77-GHz range [203]. Beyond 100-GHz, the saturating f_i/f_{\max} values of scaled CMOS make competitive designs challenging compared to SiGe. Standard approaches to increase the output power rely on massive radiator arrays [204]–[206] or a multitude of parallel frequency multipliers [207] but are limited to below 0 dBm radiated power, a value that can easily be achieved with a two-way SiGe frequency multiplier at much higher bandwidth [176]. Despite these deficits, a number of complex CMOS transceivers for IEEE 802.15.3d THz short-range data communication have been presented [208]–[210].

VI. CONCLUSION

In this invited paper, the evolution and status of integrated millimeter-wave and THz transceiver front ends in SiGe BiCMOS technologies has been reviewed. During the last decade, major commercial products in the 60- and 77-GHz range have emerged, which have sparked further research targeted toward the THz spectrum. Here, the current state-of-the-art in SiGe has reached the submillimeter-wave range around 300 GHz. Such high carrier frequencies have enabled the realization of radar sensors with a bandwidth of 60 GHz as well as wireless transceivers with data rates of 100 Gb/s. Recent successes in the proliferation of SiGe HBTs with an f_{\max} of 700 GHz will push the carrier frequencies even farther into the THz regime but also increase high-frequency performance and efficiency in the upper millimeter-wave range. Finally, emerging EPIC technologies and heterogeneous integration approaches offer new possibilities in functionality and balancing of transceiver front-end building blocks.

REFERENCES

- [1] B. Brar, G. J. Sullivan, and P. M. Asbeck, "Herb's bipolar transistor," *IEEE Trans. Electron Devices*, vol. 48, no. 11, pp. 2473–2476, Nov. 2001.
- [2] H. Kroemer, "Theory of a wide-gap emitter for transistors," *Proc. IRE*, vol. 45, no. 11, pp. 1535–1537, Nov. 1957.
- [3] E. Kasper, H. J. Herzog, and H. Kibbel, "A one-dimensional SiGe superlattice grown by UHV epitaxy," *Appl. Phys.*, vol. 8, pp. 199–205, Nov. 1975.
- [4] B. Sadhu, X. Gu, and A. Valdes-Garcia, "The more (antennas), the merrier: A survey of silicon-based mm-wave phased arrays using multi-IC scaling," *IEEE Microw. Mag.*, vol. 20, no. 12, pp. 32–50, Dec. 2019.
- [5] J. W. May and G. M. Rebeiz, "Design and characterization of W-band SiGe RFICs for passive millimeter-wave imaging," *IEEE Trans. Microw. Theory Techn.*, vol. 58, no. 5, pp. 1420–1430, May 2010.
- [6] Z. Chen, C. Wang, H. Yao, and P. Heydari, "A BiCMOS W-band 2×2 focal-plane array with on-chip antenna," *IEEE J. Solid-State Circuits*, vol. 47, no. 10, pp. 2355–2371, Oct. 2012.
- [7] E. Dacquay *et al.*, "D-band total power radiometer performance optimization in a SiGe HBT technology," *IEEE Trans. Microw. Theory Techn.*, vol. 60, no. 3, pp. 813–826, Mar. 2012.
- [8] P. Hillger, J. Grzyb, R. Jain, and U. R. Pfeiffer, "Terahertz imaging and sensing applications with silicon-based technologies," *IEEE Trans. THz Sci. Technol.*, vol. 9, no. 1, pp. 1–19, Jan. 2019.
- [9] K. Schmalz *et al.*, "245-GHz transmitter array in SiGe BiCMOS for gas spectroscopy," *IEEE Trans. THz Sci. Technol.*, vol. 6, no. 2, pp. 318–327, Mar. 2016.
- [10] N. Rothbart, K. Schmalz, J. Borngraber, D. Kissinger, and H.-W. Hubers, "Gas spectroscopy by voltage-frequency tuning of a 245 GHz SiGe transmitter and receiver," *IEEE Sensors J.*, vol. 16, no. 24, pp. 8863–8864, Dec. 2016.
- [11] K. Schmalz, N. Rothbart, P. F.-X. Neumaier, J. Borngraber, H.-W. Hubers, and D. Kissinger, "Gas spectroscopy system for breath analysis at mm-wave/THz using SiGe BiCMOS circuits," *IEEE Trans. Microw. Theory Techn.*, vol. 65, no. 5, pp. 1807–1818, May 2017.
- [12] B. Laemmle, K. Schmalz, J. C. Scheytt, R. Weigel, and D. Kissinger, "A 125-GHz permittivity sensor with read-out circuit in a 250-nm SiGe BiCMOS technology," *IEEE Trans. Microw. Theory Techn.*, vol. 61, no. 5, pp. 2185–2194, May 2013.
- [13] I. Nasr, J. Nehring, K. Aufinger, G. Fischer, R. Weigel, and D. Kissinger, "Single and dual-port 50–100-GHz highly integrated vector network analyzers with on-chip dielectric sensors," *IEEE Trans. Microw. Theory Techn.*, vol. 62, no. 9, pp. 2168–2179, Sep. 2014.
- [14] J. Nehring, M. Dietz, K. Aufinger, G. Fischer, R. Weigel, and D. Kissinger, "A 4–32-GHz chipset for a highly integrated heterodyne two-port vector network analyzer," *IEEE Trans. Microw. Theory Techn.*, vol. 64, no. 3, pp. 892–905, Mar. 2016.
- [15] J. Nehring *et al.*, "Highly integrated 4–32-GHz two-port vector network analyzers for instrumentation and biomedical applications," *IEEE Trans. Microw. Theory Techn.*, vol. 65, no. 1, pp. 229–244, Jan. 2017.
- [16] D. Wang *et al.*, "Integrated 240-GHz dielectric sensor with DC readout circuit in a 130-nm SiGe BiCMOS technology," *IEEE Trans. Microw. Theory Techn.*, vol. 66, no. 9, pp. 4232–4241, Sep. 2018.
- [17] D. Wang *et al.*, "240-GHz four-channel power-tuning heterodyne sensing readout system with reflection and transmission measurements in a 130-nm SiGe BiCMOS technology," *IEEE Trans. Microw. Theory Techn.*, vol. 67, no. 12, pp. 5296–5306, Dec. 2019.
- [18] J. Bock *et al.*, "High-performance implanted base silicon bipolar technology for RF applications," *IEEE Trans. Electron Devices*, vol. 48, no. 11, pp. 2514–2519, Nov. 2001.
- [19] J. Korn, H. Rücker, B. Heinemann, A. Pawlak, G. Wedel, and M. Schröter, "Experimental and theoretical study of f_T for SiGe HBTs with a scaled vertical doping profile," in *Proc. Bipolar/BiCMOS Circuits Technol. Meeting*, Boston, MA, USA, Oct. 2015, pp. 117–120.
- [20] D. A. Neamen, *Semiconductor Physics and Devices—Basic Principles*, 4th ed. New York, NY, USA: McGraw-Hill, 2011.
- [21] P. R. Gray, P. J. Hurst, S. H. Lewis, and R. G. Meyer, *Analysis and Design of Analog Integrated Circuits*, 5th ed. Hoboken, NJ, USA: Wiley, 2009.
- [22] J. D. Cressler and G. Niu, *Silicon Germanium Heterojunction Bipolar Transistors*. Norwood, MA, USA: Artech House, 2002.
- [23] A. Fox *et al.*, "Advanced heterojunction bipolar transistors for half-THz SiGe BiCMOS technology," *IEEE Electron Device Lett.*, vol. 36, no. 7, pp. 642–644, Jul. 2015.
- [24] S. P. Voignescu, *High-Frequency Integrated Circuits*. Cambridge, U.K.: Cambridge Univ. Press, 2013.
- [25] S. M. Sze and K. K. Ng, *Physics of Semiconductor Devices*, 3rd ed. Hoboken, NJ, USA: Wiley, 2008.

- [26] H. Rucker, B. Heinemann, and A. Fox, "Half-terahertz SiGe BiCMOS technology," in *Proc. IEEE Silicon Monolithic Integr. Circuits RF Syst.*, Santa Clara, CA, USA, Jan. 2012, pp. 133–136.
- [27] P. Chevalier *et al.*, "SiGe BiCMOS current status and future trends in Europe," in *Proc. IEEE BiCMOS Compound Semiconductor Integr. Circuits Technol. Symp. (BCICTS)*, San Diego, CA, USA, Oct. 2018, pp. 64–71.
- [28] B. Heinemann *et al.*, "SiGe HBT with f_t/f_{max} of 505 GHz/720 GHz," in *IEDM Tech. Dig.*, San Francisco, CA, USA, Dec. 2016, pp. 1–4.
- [29] P. Chevalier *et al.*, "A 55 nm triple gate oxide 9 metal layers SiGe BiCMOS technology featuring 320 GHz f_T / 370 GHz f_{MAX} HBT and high-Q millimeter-wave passives," in *IEDM Tech. Dig.*, San Francisco, CA, USA, Dec. 2014, pp. 1–3.
- [30] E. Preisler *et al.*, "A millimeter-wave capable SiGe BiCMOS process with 270 GHz f_{max} HBTs designed for high volume manufacturing," in *Proc. Bipolar/BiCMOS Circuits Technol. Meeting*, Atlanta, GA, USA, Oct. 2011, pp. 74–78.
- [31] J. J. Pekarik *et al.*, "A 90 nm SiGe BiCMOS technology for mm-wave and high-performance analog applications," in *Proc. Bipolar/BiCMOS Circuits Technol. Meeting*, Coronado, CA, USA, Sep. 2014, pp. 92–95.
- [32] P. Chevalier *et al.*, "Si/SiGe:C and InP/GaAsSb heterojunction bipolar transistors for THz applications," *Proc. IEEE*, vol. 105, no. 6, pp. 1035–1050, Jun. 2017.
- [33] H. Rucker and B. Heinemann, "Device architectures for high-speed SiGe HBTs," in *Proc. IEEE BiCMOS Compound Semiconductor Integr. Circuits Technol. Symp.*, Nashville, TN, USA, Nov. 2019, pp. 1–7.
- [34] H.-P. Forstner *et al.*, "A 77 GHz 4-channel automotive radar transceiver in SiGe," in *Proc. IEEE Radio Freq. Integr. Circuits Symp.*, Atlanta, GA, USA, Jun. 2008, pp. 233–236.
- [35] H. Knapp *et al.*, "Three-channel 77 GHz automotive radar transmitter in plastic package," in *Proc. IEEE Radio Freq. Integr. Circuits Symp.*, Montreal, QC, Canada, Jun. 2012, pp. 119–122.
- [36] C. Wagner *et al.*, "A 77 GHz automotive radar receiver in a wafer level package," in *Proc. IEEE Radio Freq. Integr. Circuits Symp.*, Montreal, QC, Canada, Jun. 2012, pp. 511–514.
- [37] M. Kucharski, A. Ergintav, W. A. Ahmad, M. Krstic, H. J. Ng, and D. Kissinger, "A scalable 79-GHz radar platform based on single-channel transceivers," *IEEE Trans. Microw. Theory Techn.*, vol. 67, no. 9, pp. 3882–3896, Sep. 2019.
- [38] J. Hasch, E. Topak, R. Schnabel, T. Zwick, R. Weigel, and C. Waldschmidt, "Millimeter-wave technology for automotive radar sensors in the 77 GHz frequency band," *IEEE Trans. Microw. Theory Techn.*, vol. 60, no. 3, pp. 845–860, Mar. 2012.
- [39] H. Li and H.-M. Rein, "Millimeter-wave VCOs with wide tuning range and low phase noise, fully integrated in a SiGe bipolar production technology," *IEEE J. Solid-State Circuits*, vol. 38, no. 2, pp. 184–191, Feb. 2003.
- [40] H. Li, H.-M. Rein, T. Suttorp, and J. Bock, "Fully integrated SiGe VCOs with powerful output buffer for 77-GHz automotive radar systems and applications around 100 GHz," *IEEE J. Solid-State Circuits*, vol. 39, no. 10, pp. 1650–1658, Oct. 2004.
- [41] S. T. Nicolson *et al.*, "Design and scaling of W-band SiGe BiCMOS VCOs," *IEEE J. Solid-State Circuits*, vol. 42, no. 9, pp. 1821–1833, Sep. 2007.
- [42] N. Pohl, H.-M. Rein, T. Musch, K. Aufinger, and J. Hausner, "SiGe bipolar VCO with ultra-wide tuning range at 80 GHz center frequency," *IEEE J. Solid-State Circuits*, vol. 44, no. 10, pp. 2655–2662, Oct. 2009.
- [43] A. Komijani and A. Hajimiri, "A wideband 77-GHz, 17.5-dBm fully integrated power amplifier in silicon," *IEEE J. Solid-State Circuits*, vol. 41, no. 8, pp. 1749–1756, Aug. 2006.
- [44] V. Giammello, E. Ragonese, and G. Palmisano, "A 15-dBm SiGe BiCMOS PA for 77-GHz automotive radar," *IEEE Trans. Microw. Theory Techn.*, vol. 59, no. 11, pp. 2910–2918, Nov. 2011.
- [45] Y. Zhao and J. R. Long, "A wideband, dual-path, millimeter-wave power amplifier with 20 dBm output power and PAE above 15% in 130 nm SiGe-BiCMOS," *IEEE J. Solid-State Circuits*, vol. 47, no. 9, pp. 1981–1997, Sep. 2012.
- [46] M. Thian, M. Tiebout, N. B. Buchanan, V. F. Fusco, and F. Dielacher, "A 76–84 GHz SiGe power amplifier array employing low-loss four-way differential combining transformer," *IEEE Trans. Microw. Theory Techn.*, vol. 61, no. 2, pp. 931–938, Feb. 2013.
- [47] S. T. Nicolson *et al.*, "A low-voltage SiGe BiCMOS 77-GHz automotive radar chipset," *IEEE Trans. Microw. Theory Techn.*, vol. 56, no. 5, pp. 1092–1104, May 2008.
- [48] E. Kasper, D. Kissinger, P. Russer, and R. Weigel, "High speeds in a single chip," *IEEE Microw. Mag.*, vol. 10, no. 7, pp. 28–33, Dec. 2009.
- [49] A. Natarajan, A. Komijani, X. Guan, A. Babakhani, and A. Hajimiri, "A 77-GHz phased-array transceiver with on-chip antennas in silicon: Transmitter and local lo-path phase shifting," *IEEE J. Solid-State Circuits*, vol. 41, no. 12, pp. 2807–2819, Dec. 2006.
- [50] A. Babakhani, G. Xiang, A. Komijani, A. Natarajan, and A. Hajimiri, "A 77-GHz phased-array transceiver with on-chip antennas in silicon: Receiver and antennas," *IEEE J. Solid-State Circuits*, vol. 41, no. 12, pp. 2795–2806, Dec. 2006.
- [51] S. T. Nicolson, P. Chevalier, B. Sautreuil, and S. P. Voinescu, "Single-chip W-band SiGe HBT transceivers and receivers for Doppler radar and millimeter-wave imaging," *IEEE J. Solid-State Circuits*, vol. 43, no. 10, pp. 2206–2217, Oct. 2008.
- [52] R. Feger, C. Wagner, S. Schuster, S. Scheibelhofer, H. Jager, and A. Stelzer, "A 77-GHz FMCW MIMO radar based on an SiGe single-chip transceiver," *IEEE Trans. Microw. Theory Techn.*, vol. 57, no. 5, pp. 1020–1035, May 2009.
- [53] V. Jain, F. Tzeng, L. Zhou, and P. Heydari, "A single-chip dual-band 22–29-GHz/77–81 GHz BiCMOS transceiver for automotive radars," *IEEE J. Solid-State Circuits*, vol. 44, no. 12, pp. 3469–3485, Dec. 2009.
- [54] M. Wojnowski, C. Wagner, R. Lachner, J. Böck, G. Sommer, and K. Pressel, "A 77-GHz SiGe single-chip four-channel transceiver module with integrated antennas in embedded wafer-level BGA package," in *Proc. Electron. Compon. Technol. Conf.*, San Diego, CA, USA, May 2012, pp. 1027–1032.
- [55] S. Trotta *et al.*, "An RCP packaged transceiver chipset for automotive LRR and SRR systems in SiGe BiCMOS technology," *IEEE Trans. Microw. Theory Techn.*, vol. 60, no. 3, pp. 778–794, Mar. 2012.
- [56] T. Fujibayashi *et al.*, "A 76- to 81-GHz multi-channel radar transceiver," *IEEE J. Solid-State Circuits*, vol. 52, no. 9, pp. 2226–2241, Sep. 2017.
- [57] R. Feger, C. Pfeffer, and A. Stelzer, "A frequency-division MIMO FMCW radar system based on delta-sigma modulated transmitters," *IEEE Trans. Microw. Theory Techn.*, vol. 62, no. 12, pp. 3572–3581, Dec. 2014.
- [58] S. Trotta *et al.*, "A 79 GHz SiGe-bipolar spread-spectrum TX for automotive radar," in *IEEE Int. Solid-State Circuits Conf. (ISSCC) Dig. Tech. Papers*, San Francisco, CA, USA, Feb. 2007, pp. 430–431.
- [59] H. Ng, R. Feger, and A. Stelzer, "A fully-integrated 77-GHz UWB pseudo-random noise radar transceiver with a programmable sequence generator in SiGe technology," *IEEE Trans. Circuits Syst. I, Reg. Papers*, vol. 61, no. 8, pp. 2444–2455, Aug. 2014.
- [60] S. Y. Kim and G. M. Rebeiz, "A low-power BiCMOS 4-element phased array receiver for 76–84 GHz radars and communication systems," *IEEE J. Solid-State Circuits*, vol. 47, no. 2, pp. 359–367, Feb. 2012.
- [61] B.-H. Ku, O. Inac, M. Chang, H.-H. Yang, and G. M. Rebeiz, "A high-linearity 76–85-GHz 16-element 8-transmit/8-receive phased-array chip with high isolation and flip-chip packaging," *IEEE Trans. Microw. Theory Techn.*, vol. 62, no. 10, pp. 2337–2356, Oct. 2014.
- [62] B.-H. Ku *et al.*, "A 77–81-GHz 16-element phased-array receiver with $\pm 50^\circ$ beam scanning for advanced automotive radars," *IEEE Trans. Microw. Theory Techn.*, vol. 62, no. 11, pp. 2823–2832, Nov. 2014.
- [63] C. Wagner, H.-P. Forstner, G. Haider, A. Stelzer, and H. Jäger, "A 79-GHz radar transceiver with switchable TX and LO feedthrough in a silicon-germanium technology," in *Proc. Bipolar/BiCMOS Circuits Technol. Meeting*, Monterey, CA, USA, Oct. 2008, pp. 105–108.
- [64] C. Wagner, A. Stelzer, and H. Jäger, "A phased-array radar transmitter based on 77-GHz cascaded transceivers," in *IEEE MTT-S Int. Microw. Symp. Dig.*, Boston, MA, USA, Jun. 2009, pp. 73–76.
- [65] E. Öztürk, U. Yodprasit, D. Kissinger, W. Winkler, and W. Debski, "A master/slave 55.5–64.8 GHz 4×4 FMCW radar transceiver in 130 nm SiGe BiCMOS for massive MIMO applications," in *IEEE MTT-S Int. Microw. Symp. Dig.*, Boston, MA, USA, Jun. 2019, pp. 683–686.
- [66] C. Beck *et al.*, "Industrial mmWave radar sensor in embedded wafer-level BGA packaging technology," *IEEE Sensors J.*, vol. 16, no. 17, pp. 6566–6578, Sep. 2016.
- [67] H. J. Ng, M. Kucharski, W. Ahmad, and D. Kissinger, "Multi-purpose fully-differential 61- and 122-GHz radar transceivers for scalable MIMO sensor platforms," *IEEE J. Solid-State Circuits*, vol. 52, no. 9, pp. 2242–2255, Sep. 2017.
- [68] M. Frank *et al.*, "Antenna and package design for 61- and 122-GHz radar sensors in embedded wafer-level ball grid array technology," *IEEE Trans. Microw. Theory Techn.*, vol. 66, no. 12, pp. 5156–5168, Dec. 2018.

- [69] H. J. Ng, R. Feger, and D. Kissinger, "Scalable mm-Wave 4-channel radar SoC with vector modulators and demodulators for MIMO and phased array applications," in *IEEE MTT-S Int. Microw. Symp. Dig.*, Philadelphia, PA, USA, Jun. 2018, pp. 1472–1475.
- [70] I. Nasr, M. Dudek, R. Weigel, and D. Kissinger, "A 33% tuning range high output power V-band superharmonic coupled quadrature VCO in SiGe technology," in *Proc. IEEE Radio Freq. Integr. Circuits Symp.*, Montreal, QC, Canada, Jun. 2012, pp. 301–304.
- [71] N. Pohl, T. Klein, K. Aufinger, and H.-M. Rein, "A low-power wideband transmitter front-end chip for 80 GHz FMCW radar systems with integrated 23 GHz downconverter VCO," *IEEE J. Solid-State Circuits*, vol. 47, no. 9, pp. 1974–1980, Sep. 2012.
- [72] N. Pohl, T. Jaeschke, and K. Aufinger, "An ultra-wideband 80 GHz FMCW radar system using a SiGe bipolar transceiver chip stabilized by a fractional-N PLL synthesizer," *IEEE Trans. Microw. Theory Techn.*, vol. 60, no. 3, pp. 757–765, Mar. 2012.
- [73] M. Jahn, R. Feger, C. Wagner, Z. Tong, and A. Stelzer, "A four-channel 94-GHz SiGe-based digital beamforming FMCW radar," *IEEE Trans. Microw. Theory Techn.*, vol. 60, no. 3, pp. 861–869, Mar. 2012.
- [74] A. Arbabian, S. Callender, S. Kang, M. Rangwala, and A. M. Niknejad, "A 94 GHz mm-wave-to-baseband pulsed-radar transceiver with applications in imaging and gesture recognition," *IEEE J. Solid-State Circuits*, vol. 48, no. 4, pp. 1055–1071, Apr. 2013.
- [75] F. Golcuk, T. Kanar, and G. M. Rebeiz, "A 90–100-GHz 4×4 SiGe BiCMOS polarimetric transmit/receive phased array with simultaneous receive-beams capabilities," *IEEE Trans. Microw. Theory Techn.*, vol. 61, no. 8, pp. 3099–3114, Aug. 2013.
- [76] O. Inac, F. Golcuk, T. Kanar, and G. M. Rebeiz, "A 90–100-GHz phased-array transmit/receive silicon RFIC module with built-in self-test," *IEEE Trans. Microw. Theory Techn.*, vol. 61, no. 10, pp. 3774–3782, Oct. 2013.
- [77] A. Townley *et al.*, "A 94-GHz 4 TX-4 RX phased-array FMCW radar transceiver with antenna-in-package," *IEEE J. Solid-State Circuits*, vol. 52, no. 5, pp. 1245–1259, May 2017.
- [78] B. Welp *et al.*, "Versatile dual-receiver 94-GHz FMCW radar system with high output power and 26-GHz tuning range for high distance applications," *IEEE Trans. Microw. Theory Techn.*, vol. 68, no. 3, pp. 1195–1211, Mar. 2020.
- [79] E. Ozturk *et al.*, "Measuring target range and velocity: Developments in chip, antenna, and packaging technologies for 60-GHz and 122-GHz industrial radars," *IEEE Microw. Mag.*, vol. 18, no. 7, pp. 26–39, Nov. 2017.
- [80] I. M. Milosavljević *et al.*, "A SiGe highly integrated FMCW transmitter module with a 59.5–70.5-GHz single sweep cover," *IEEE Trans. Microw. Theory Techn.*, vol. 66, no. 9, pp. 4121–4133, Sep. 2018.
- [81] E. Öztürk *et al.*, "A 60-GHz SiGe BiCMOS monostatic transceiver for FMCW radar applications," *IEEE Trans. Microw. Theory Techn.*, vol. 65, no. 12, pp. 5309–5323, Dec. 2017.
- [82] C. Bredendiek *et al.*, "A 61-GHz SiGe transceiver frontend for energy and data transmission of passive RFID single-chip tags with integrated antennas," *IEEE J. Solid-State Circuits*, vol. 53, no. 9, pp. 2441–2453, Sep. 2018.
- [83] A. Hagelauer, M. Wojnowski, K. Pressel, R. Weigel, and D. Kissinger, "Integrated systems-in-package: Heterogeneous integration of millimeter-wave active circuits and passives in fan-out wafer-level packaging technologies," *IEEE Microw. Mag.*, vol. 19, no. 1, pp. 48–56, Jan. 2018.
- [84] I. Nasr *et al.*, "A highly integrated 60 GHz 6-channel transceiver with antenna in package for smart sensing and short-range communications," *IEEE J. Solid-State Circuits*, vol. 51, no. 9, pp. 2066–2076, Sep. 2016.
- [85] H. Lin and G. M. Rebeiz, "A 110–134-GHz SiGe amplifier with peak output power of 100–120 mW," *IEEE Trans. Microw. Theory Techn.*, vol. 62, no. 12, pp. 2990–3000, Dec. 2014.
- [86] S. Daneshgar and J. F. Buckwalter, "Compact series power combining using subquarter-wavelength baluns in silicon germanium at 120 GHz," *IEEE Trans. Microw. Theory Techn.*, vol. 66, no. 11, pp. 4844–4859, Nov. 2018.
- [87] M. Furqan, F. Ahmed, K. Aufinger, and A. Stelzer, "A D-band fully-differential quadrature FMCW radar transceiver with 11 dBm output power and a 3-dB 30-GHz bandwidth in SiGe BiCMOS," in *IEEE MTT-S Int. Microw. Symp. Dig.*, Honolulu, HI, USA, Jun. 2017, pp. 1404–1407.
- [88] H. J. Ng, R. Hasan, and D. Kissinger, "A scalable four-channel frequency-division multiplexing MIMO radar utilizing single-sideband delta-sigma modulation," *IEEE Trans. Microw. Theory Techn.*, vol. 67, no. 11, pp. 4578–4590, Nov. 2019.
- [89] Y. Sun *et al.*, "A low-cost miniature 120 GHz SiP FMCW/CW radar sensor with software linearization," in *IEEE Int. Solid-State Circuits Conf. (ISSCC) Dig. Tech. Papers*, Feb. 2013, pp. 148–149.
- [90] T. Zwick, F. Boes, B. Göttel, A. Bhutani, and M. Pauli, "Pea-sized mmW transceivers: QFN-based packaging concepts for millimeter-wave transceivers," *IEEE Microw. Mag.*, vol. 18, no. 6, pp. 79–89, Sep. 2017.
- [91] I. Sarkas, J. Hasch, A. Balteanu, and S. P. Voinescu, "A fundamental frequency 120-GHz SiGe BiCMOS distance sensor with integrated antenna," *IEEE Trans. Microw. Theory Techn.*, vol. 60, no. 3, pp. 795–812, Mar. 2012.
- [92] H. J. Ng and D. Kissinger, "Highly miniaturized 120-GHz SIMO and MIMO radar sensor with on-chip folded dipole antennas for range and angular measurements," *IEEE Trans. Microw. Theory Techn.*, vol. 66, no. 6, pp. 2592–2603, Jun. 2018.
- [93] M. Kucharski, H. J. Ng, and D. Kissinger, "An 18 dBm 155–180 GHz SiGe power amplifier using a 4-way T-junction combining network," in *Proc. Eur. Solid-State Circuits Conf.*, Krakow, Poland, Sep. 2019, pp. 333–336.
- [94] W. A. Ahmad *et al.*, "Multimode W-band and D-band MIMO scalable radar platform," *IEEE Trans. Microw. Theory Techn.*, vol. 69, no. 1, pp. 1036–1047, Jan. 2021.
- [95] M. Kucharski, M. H. Eissa, A. Malignaggi, D. Wang, H. J. Ng, and D. Kissinger, "D-band frequency quadruplers in BiCMOS technology," *IEEE J. Solid-State Circuits*, vol. 53, no. 9, pp. 2465–2478, Sep. 2018.
- [96] N. Sarmah, P. Chevalier, and U. R. Pfeiffer, "160-GHz power amplifier design in advanced SiGe HBT technologies with P_{sat} in excess of 10 dBm," *IEEE Trans. Microw. Theory Techn.*, vol. 61, no. 2, pp. 939–947, Feb. 2013.
- [97] M. Furqan, F. Ahmed, B. Heinemann, and A. Stelzer, "A 15.5-dBm 160-GHz high-gain power amplifier in SiGe BiCMOS technology," *IEEE Microw. Wireless Compon. Lett.*, vol. 27, no. 2, pp. 177–179, Feb. 2017.
- [98] M. Jahn, R. Feger, C. Pfeiffer, T. F. Meister, and A. Stelzer, "A SiGe-based 140-GHz four-channel radar sensor with digital beamforming capability," in *IEEE MTT-S Int. Microw. Symp. Dig.*, Montreal, QC, Canada, Jun. 2012, pp. 1–3.
- [99] E. Laskin, P. Chevalier, A. Chantre, B. Sautreuil, and S. P. Voinescu, "165-GHz transceiver in SiGe technology," *IEEE J. Solid-State Circuits*, vol. 43, no. 5, pp. 1087–1100, May 2008.
- [100] A. Hamidipour, A. Fischer, M. Jahn, and A. Stelzer, "160-GHz SiGe-based transmitter and receiver with highly directional antennas in package," in *Proc. Eur. Microw. Integr. Circuits Conf.*, Nuremberg, Germany, Oct. 2013, pp. 81–84.
- [101] M. Hitzler *et al.*, "Ultrapact 160-GHz FMCW radar MMIC with fully integrated offset synthesizer," *IEEE Trans. Microw. Theory Techn.*, vol. 65, no. 5, pp. 1682–1691, May 2017.
- [102] A. Dürr *et al.*, "High-resolution 160-GHz imaging MIMO radar using MMICs with on-chip frequency synthesizers," *IEEE Trans. Microw. Theory Techn.*, vol. 67, no. 9, pp. 3897–3907, Sep. 2019.
- [103] T. Jaeschke, C. Bredendiek, S. Küppers, and N. Pohl, "High-precision D-band FMCW-radar sensor based on a wideband SiGe-transceiver MMIC," *IEEE Trans. Microw. Theory Techn.*, vol. 62, no. 12, pp. 3582–3597, Dec. 2014.
- [104] S. Yuan, A. Trasser, and H. Schumacher, "56 GHz bandwidth FMCW radar sensor with on-chip antennas in SiGe BiCMOS," in *IEEE MTT-S Int. Microw. Symp. Dig.*, Tampa, FL, USA, Jun. 2014, pp. 1–4.
- [105] A. Ali, J. Yun, M. Kucharski, H. J. Ng, D. Kissinger, and P. Colantonio, "220–360-GHz broadband frequency multiplier chains ($\times 8$) in 130-nm BiCMOS technology," *IEEE Trans. Microw. Theory Techn.*, vol. 68, no. 7, pp. 2701–2715, Jul. 2020.
- [106] M. Kucharski, W. A. Ahmad, H. J. Ng, and D. Kissinger, "Monostatic and bistatic G-band BiCMOS radar transceivers with on-chip antennas and tunable TX-to-RX leakage cancellation," *IEEE J. Solid-State Circuits*, vol. 56, no. 3, pp. 899–913, Mar. 2021.
- [107] E. Öjefors, B. Heinemann, and U. R. Pfeiffer, "Active 220- and 325-GHz frequency multiplier chains in an SiGe HBT technology," *IEEE Trans. Microw. Theory Techn.*, vol. 59, no. 5, pp. 1311–1318, May 2011.

- [108] P. Zhou, J. Chen, P. Yan, Z. Chen, D. Hou, and W. Hong, "A 273.5–312-GHz signal source with 2.3 dBm peak output power in a 130-nm SiGe BiCMOS process," *IEEE Trans. THz Sci. Technol.*, vol. 10, no. 3, pp. 260–270, May 2020.
- [109] S. P. Voinigescu *et al.*, "A study of SiGe HBT signal sources in the 220–330-GHz range," *IEEE J. Solid-State Circuits*, vol. 48, no. 9, pp. 2011–2021, Sep. 2013.
- [110] J. Yun, D. Yoon, S. Jung, M. Kaynak, B. Tillack, and J. Rieh, "Two 320 GHz signal sources based on SiGe HBT technology," *IEEE Microw. Wireless Compon. Lett.*, vol. 25, no. 3, pp. 178–180, Mar. 2015.
- [111] F. Ahmed, M. Furqan, B. Heinemann, and A. Stelzer, "0.3-THz SiGe-based high-efficiency push–push VCOs with > 1-mW peak output power employing common-mode impedance enhancement," *IEEE Trans. Microw. Theory Techn.*, vol. 66, no. 3, pp. 1384–1398, Mar. 2018.
- [112] R. Han *et al.*, "A SiGe terahertz heterodyne imaging transmitter with 3.3 mW radiated power and fully-integrated phase-locked loop," *IEEE J. Solid-State Circuits*, vol. 50, no. 12, pp. 2935–2947, Dec. 2015.
- [113] H. Jalili and O. Momeni, "A 0.34-THz wideband wide-angle 2-D steering phased array in 0.13- μ m SiGe BiCMOS," *IEEE J. Solid-State Circuits*, vol. 54, no. 9, pp. 2449–2461, Sep. 2019.
- [114] C. Jiang *et al.*, "A fully integrated 320 GHz coherent imaging transceiver in 130 nm SiGe BiCMOS," *IEEE J. Solid-State Circuits*, vol. 51, no. 11, pp. 2596–2609, Nov. 2016.
- [115] E. Ojefors, B. Heinemann, and U. R. Pfeiffer, "Subharmonic 220- and 320-GHz SiGe HBT receiver front-ends," *IEEE Trans. Microw. Theory Techn.*, vol. 60, no. 5, pp. 1397–1404, May 2012.
- [116] A. Mostajeran, A. Cathelin, and E. Afshari, "A 170-GHz fully integrated single-chip FMCW imaging radar with 3-D imaging capability," *IEEE J. Solid-State Circuits*, vol. 52, no. 10, pp. 2721–2734, Oct. 2017.
- [117] J. Grzyb, K. Statnikov, N. Sarmah, B. Heinemann, and U. R. Pfeiffer, "A 210–270-GHz circularly polarized FMCW radar with a single-lens-coupled SiGe HBT chip," *IEEE Trans. THz Sci. Technol.*, vol. 6, no. 6, pp. 771–783, Nov. 2016.
- [118] S. Thomas, C. Bredendiek, and N. Pohl, "A SiGe-based 240-GHz FMCW radar system for high-resolution measurements," *IEEE Trans. Microw. Theory Techn.*, vol. 67, no. 11, pp. 4599–4609, Nov. 2019.
- [119] J.-D. Park, S. Kang, and A. M. Niknejad, "A 0.38 THz fully integrated transceiver utilizing a quadrature push-push harmonic circuitry in SiGe BiCMOS," *IEEE J. Solid-State Circuits*, vol. 47, no. 10, pp. 2344–2354, Oct. 2012.
- [120] J. Al-Eryani, H. Knapp, J. Kammerer, K. Aufinger, H. Li, and L. Maurer, "Fully integrated single-chip 305–375-GHz transceiver with on-chip antennas in SiGe BiCMOS," *IEEE Trans. THz Sci. Technol.*, vol. 8, no. 3, pp. 329–339, May 2018.
- [121] A. Malignaggi, M. Ko, M. Elkhoully, and D. Kissinger, "A scalable 8-channel bidirectional V-band beamformer in 130 nm SiGe:C BiCMOS technology," in *IEEE MTT-S Int. Microw. Symp. Dig.*, Honolulu, HI, USA, Jun. 2017, pp. 1–4.
- [122] A. Gadallah, A. Franzese, M. H. Eissa, K. Drenkhahn, D. Kissinger, and A. Malignaggi, "A 4-channel V-band beamformer featuring a switchless PALNA for scalable phased array systems," in *IEEE MTT-S Int. Microw. Symp. Dig.*, Atlanta, GA, USA, Jun. 2021, pp. 839–841.
- [123] A. Gadallah, M. H. Eissa, D. Kissinger, and A. Malignaggi, "A V-band miniaturized bidirectional switchless PALNA in SiGe:C BiCMOS technology," *IEEE Microw. Wireless Compon. Lett.*, vol. 30, no. 8, pp. 786–789, Aug. 2020.
- [124] B. A. Floyd, S. K. Reynolds, U. R. Pfeiffer, T. Zwick, T. Beukema, and B. Gaucher, "SiGe bipolar transceiver circuits operating at 60 GHz," *IEEE J. Solid-State Circuits*, vol. 40, no. 1, pp. 156–167, Jan. 2005.
- [125] S. K. Reynolds *et al.*, "A silicon 60-GHz receiver and transmitter chipset for broadband communications," *IEEE J. Solid-State Circuits*, vol. 41, no. 12, pp. 2820–2831, Dec. 2006.
- [126] U. R. Pfeiffer and D. Goren, "A 23-dBm 60-GHz distributed active transformer in a silicon process technology," *IEEE Trans. Microw. Theory Techn.*, vol. 55, no. 5, pp. 857–865, May 2007.
- [127] U. R. Pfeiffer *et al.*, "A chip-scale packaging technology for 60-GHz wireless chipsets," *IEEE Trans. Microw. Theory Techn.*, vol. 54, no. 8, pp. 3387–3397, Aug. 2006.
- [128] A. Valdes-Garcia *et al.*, "A fully integrated 16-element phased-array transmitter in SiGe BiCMOS for 60-GHz communications," *IEEE J. Solid-State Circuits*, vol. 45, no. 12, pp. 2757–2773, Dec. 2010.
- [129] A. Natarajan *et al.*, "A fully-integrated 16-element phased-array receiver in SiGe BiCMOS for 60-GHz communications," *IEEE J. Solid-State Circuits*, vol. 46, no. 5, pp. 1059–1075, May 2011.
- [130] A. Tomkins *et al.*, "A 60 GHz, 802.11ad/WiGig-compliant transceiver for infrastructure and mobile applications in 130 nm SiGe BiCMOS," *IEEE J. Solid-State Circuits*, vol. 50, no. 10, pp. 2239–2255, Oct. 2015.
- [131] S. Zahir, O. D. Gurbuz, A. Kar-Roy, S. Raman, and G. M. Rebeiz, "60-GHz 64- and 256-elements wafer-scale phased-array transmitters using full-reticle and subreticle stitching techniques," *IEEE Trans. Microw. Theory Techn.*, vol. 64, no. 12, pp. 4701–4719, Dec. 2016.
- [132] B. Rupakula, A. Nafe, S. Zahir, Y. Wang, T.-W. Lin, and G. Rebeiz, "63.5–65.5-GHz transmit/receive phased-array communication link with 0.5–2 Gb/s at 100–800 m and $\pm 50^\circ$ scan angles," *IEEE Trans. Microw. Theory Techn.*, vol. 66, no. 9, pp. 4108–4120, Sep. 2018.
- [133] D. Kissinger *et al.*, "Integrated millimeter-wave transceiver concepts and technologies for wireless multi-Gbps communication," in *IEEE MTT-S Int. Microw. Symp. Dig.*, Phoenix, AZ, USA, May 2015, pp. 1–3.
- [134] I. Nasr, B. Laemmle, K. Aufinger, G. Fischer, R. Weigel, and D. Kissinger, "A 70–90-GHz high-linearity multi-band quadrature receiver in 0.35 μ m SiGe technology," *IEEE Trans. Microw. Theory Techn.*, vol. 61, no. 12, pp. 4600–4612, Dec. 2013.
- [135] I. Nasr, H. Knapp, K. Aufinger, R. Weigel, and D. Kissinger, "A 50–100-GHz highly integrated octave-bandwidth transmitter and receiver chipset in 0.35 μ m SiGe technology," *IEEE Trans. Microw. Theory Techn.*, vol. 62, no. 9, pp. 2118–2131, Sep. 2014.
- [136] H. Lin and G. M. Rebeiz, "A 70–80-GHz SiGe amplifier with peak output power of 27.3 dBm," *IEEE Trans. Microw. Theory Techn.*, vol. 64, no. 7, pp. 2039–2049, Jul. 2016.
- [137] E. Rahimi, J. Zhao, F. Svelto, and A. Mazzanti, "High-efficiency SiGe-BiCMOS E-band power amplifiers exploiting current clamping in the common-base stage," *IEEE J. Solid-State Circuits*, vol. 54, no. 8, pp. 2175–2185, Aug. 2019.
- [138] I. Sarkas *et al.*, "An 18-Gb/s, direct QPSK modulation SiGe BiCMOS transceiver for last mile links in the 70–80 GHz band," *IEEE J. Solid-State Circuits*, vol. 45, no. 10, pp. 1968–1980, Oct. 2010.
- [139] R. Levinger *et al.*, "High-performance E-band transceiver chipset for point-to-point communication in SiGe BiCMOS technology," *IEEE Trans. Microw. Theory Techn.*, vol. 64, no. 4, pp. 1078–1087, Apr. 2016.
- [140] P.-Y. Wu, T. Kijisanayotin, and J. F. Buckwalter, "A 71–86-GHz switchless asymmetric bidirectional transceiver in a 90-nm SiGe BiCMOS," *IEEE Trans. Microw. Theory Techn.*, vol. 64, no. 12, pp. 4262–4273, Dec. 2016.
- [141] T. Kijisanayotin, J. Li, and J. F. Buckwalter, "A 70-GHz LO phase-shifting bidirectional frontend using linear coupled oscillators," *IEEE Trans. Microw. Theory Techn.*, vol. 65, no. 3, pp. 892–904, Mar. 2017.
- [142] N. Ebrahimi, P.-Y. Wu, M. Bagheri, and J. F. Buckwalter, "A 71–86-GHz phased array transceiver using wideband injection-locked oscillator phase shifters," *IEEE Trans. Microw. Theory Techn.*, vol. 65, no. 2, pp. 346–361, Feb. 2017.
- [143] W. Shin, B. Ku, O. Inac, Y. Ou, and G. M. Rebeiz, "A 108–114 GHz 4 \times 4 wafer-scale phased array transmitter with high-efficiency on-chip antennas," *IEEE J. Solid-State Circuits*, vol. 48, no. 9, pp. 2041–2055, Sep. 2013.
- [144] A. Natarajan, A. Valdes-Garcia, B. Sadhu, S. K. Reynolds, and B. D. Parker, "W-band dual-polarization phased-array transceiver frontend in SiGe BiCMOS," *IEEE Trans. Microw. Theory Techn.*, vol. 63, no. 6, pp. 1989–2002, Jun. 2015.
- [145] W. Lee *et al.*, "Fully integrated 94-GHz dual-polarized TX and RX phased array chipset in SiGe BiCMOS operating up to 105 $^\circ$ C," *IEEE J. Solid-State Circuits*, vol. 53, no. 9, pp. 2512–2531, Sep. 2018.
- [146] S. Shahramian, Y. Baeyens, N. Kaneda, and Y.-K. Chen, "A 70–100 GHz direct-conversion transmitter and receiver phased array chipset demonstrating 10 Gb/s wireless link," *IEEE J. Solid-State Circuits*, vol. 48, no. 5, pp. 1113–1125, May 2013.
- [147] S. Shahramian, M. J. Holyoak, and Y. Baeyens, "A 16-element W-band phased-array transceiver chipset with flip-chip PCB integrated antennas for multi-gigabit wireless data links," *IEEE Trans. Microw. Theory Techn.*, vol. 66, no. 7, pp. 3389–3402, Jul. 2018.
- [148] S. Shahramian, M. J. Holyoak, A. Singh, and Y. Baeyens, "A fully integrated 384-element, 16-tile, W-band phased array with self-alignment and self-test," *IEEE J. Solid-State Circuits*, vol. 54, no. 9, pp. 2419–2434, Sep. 2019.

- [149] A. Karakuzulu, M. H. Eissa, D. Kissinger, and A. Malignaggi, "A broadband 110–170 GHz stagger-tuned power amplifier with 13.5-dBm P_{sat} in 130-nm SiGe," *IEEE Microw. Wireless Compon. Lett.*, vol. 31, no. 1, pp. 56–59, Jan. 2021.
- [150] A. Karakuzulu, M. H. Eissa, D. Kissinger, and A. Malignaggi, "A broadband 110–170GHz frequency multiplier by 4 chain with 8dBm output power in 130 nm BiCMOS," in *Proc. Eur. Solid-State Circuits Conf.*, Grenoble, France, Sep. 2021.
- [151] A. Karakuzulu, M. H. Eissa, D. Kissinger, and A. Malignaggi, "Full D-band transmit–receive module for phased array systems in 130-nm SiGe BiCMOS," *IEEE Solid-State Circuits Lett.*, vol. 4, pp. 40–43, Jan. 2021.
- [152] U. R. Pfeiffer, E. Öjefors, and Y. Zhao, "A SiGe quadrature transmitter and receiver chipset for emerging high-frequency applications at 160 GHz," in *IEEE Int. Solid-State Circuits Conf. (ISSCC) Dig. Tech. Papers*, San Francisco, CA, USA, Feb. 2010, pp. 416–417.
- [153] Y. Zhao, E. Ojefors, K. Aufinger, T. F. Meister, and U. R. Pfeiffer, "A 160-GHz subharmonic transmitter and receiver chipset in an SiGe HBT technology," *IEEE Trans. Microw. Theory Techn.*, vol. 60, no. 10, pp. 3286–3299, Oct. 2012.
- [154] S. Carpenter *et al.*, "A D-band 48-Gbit/s 64-QAM/QPSK direct-conversion IQ transceiver chipset," *IEEE Trans. Microw. Theory Techn.*, vol. 64, no. 4, pp. 1285–1296, Apr. 2016.
- [155] M. Elkhoully *et al.*, "D-band phased-array TX and RX front ends utilizing radio-on-glass technology," in *Proc. IEEE Radio Freq. Integr. Circuits Symp.*, Los Angeles, CA, USA, Jun. 2020, pp. 91–94.
- [156] H. Wang, H. Mohammadnezhad, and P. Heydari, "Analysis and design of high-order QAM direct-modulation transmitter for high-speed point-to-point mm-wave wireless links," *IEEE J. Solid-State Circuits*, vol. 54, no. 11, pp. 3161–3179, Nov. 2019.
- [157] H. Mohammadnezhad, H. Wang, A. Cathelin, and P. Heydari, "A 115–135-GHz 8PSK receiver using multi-phase RF-correlation-based direct-demodulation method," *IEEE J. Solid-State Circuits*, vol. 54, no. 9, pp. 2435–2448, Sep. 2019.
- [158] M. H. Eissa and D. Kissinger, "A 13.5 dBm fully integrated 200–255 GHz power amplifier with a 4-way power combiner in SiGe:C BiCMOS," in *IEEE Int. Solid-State Circuits Conf. (ISSCC) Dig. Tech. Papers*, San Francisco, CA, USA, Feb. 2019, pp. 82–83.
- [159] M. H. Eissa, A. Malignaggi, and D. Kissinger, "A 13.5-dBm 200–255-GHz 4-way power amplifier and frequency source in 130-nm BiCMOS," *IEEE Solid-State Circuits Lett.*, vol. 2, no. 11, pp. 268–271, Nov. 2019.
- [160] M. H. Eissa, N. Maletic, E. Grass, R. Kraemer, D. Kissinger, and A. Malignaggi, "100 Gbps 0.8-m wireless link based on fully integrated 240 GHz IQ transmitter and receiver," in *IEEE MTT-S Int. Microw. Symp. Dig.*, Los Angeles, CA, USA, Jun. 2020, pp. 627–630.
- [161] S. Hu *et al.*, "A SiGe BiCMOS transmitter/receiver chipset with on-chip SIW antennas for terahertz applications," *IEEE J. Solid-State Circuits*, vol. 47, no. 11, pp. 2654–2664, Nov. 2012.
- [162] X. Deng, Y. Li, J. Li, C. Liu, W. Wu, and Y. Xiong, "A 320-GHz 1×4 fully integrated phased array transmitter using 0.13- μm SiGe BiCMOS technology," *IEEE Trans. THz Sci. Technol.*, vol. 5, no. 6, pp. 930–940, Nov. 2015.
- [163] S. Shopov, A. Balteanu, J. Hasch, P. Chevalier, A. Cathelin, and P. S. Voignescu, "A 234–261-GHz 55-nm SiGe BiCMOS signal source with 5.4–7.2 dBm output power, 1.3% DC-to-RF efficiency, and 1-GHz divided-down output," *IEEE J. Solid-State Circuits*, vol. 51, no. 9, pp. 2054–2065, Sep. 2016.
- [164] H. Lin and G. M. Rebeiz, "A SiGe multiplier array with output power of 5–8 dBm at 200–230 GHz," *IEEE Trans. Microw. Theory Techn.*, vol. 64, no. 7, pp. 2050–2058, Jul. 2016.
- [165] K. Wu, S. Muralidharan, and M. M. Hella, "A wideband SiGe BiCMOS frequency doubler with 6.5-dBm peak output power for millimeter-wave signal sources," *IEEE Trans. Microw. Theory Techn.*, vol. 66, no. 1, pp. 187–200, Jan. 2018.
- [166] P. Stärke, C. Carta, and F. Ellinger, "High-linearity 19-dB power amplifier for 140–220 GHz, saturated at 15 dBm, in 130-nm SiGe," *IEEE Microw. Wireless Compon. Lett.*, vol. 30, no. 4, pp. 403–406, Apr. 2020.
- [167] N. Sarmah *et al.*, "A fully integrated 240-GHz direct-conversion quadrature transmitter and receiver chipset in SiGe technology," *IEEE Trans. Microw. Theory Techn.*, vol. 64, no. 2, pp. 562–574, Feb. 2016.
- [168] D. Fritsche, P. Stärke, C. Carta, and F. Ellinger, "A low-power SiGe BiCMOS 190-GHz transceiver chipset with demonstrated data rates up to 50 Gbit/s using on-chip antennas," *IEEE Trans. Microw. Theory Techn.*, vol. 65, no. 9, pp. 3312–3323, Sep. 2017.
- [169] M. H. Eissa *et al.*, "Wideband 240-GHz transmitter and receiver in BiCMOS technology with 25-Gbit/s data rate," *IEEE J. Solid-State Circuits*, vol. 53, no. 9, pp. 2532–2542, Sep. 2018.
- [170] U. Alakusu, M. S. Dadash, S. Shopov, P. Chevalier, A. Cathelin, and P. S. Voignescu, "A 210–284-GHz I–Q receiver with on-chip VCO and divider chain," *IEEE Microw. Wireless Compon. Lett.*, vol. 30, no. 1, pp. 50–53, Jan. 2020.
- [171] M. H. Eissa *et al.*, "Frequency interleaving IF transmitter and receiver for 240-GHz communication in SiGe:C BiCMOS," *IEEE Trans. Microw. Theory Techn.*, vol. 68, no. 1, pp. 239–251, Jan. 2020.
- [172] P. Rodriguez-Vazquez, J. Grzyb, B. Heinemann, and U. R. Pfeiffer, "A 16-QAM 100-Gb/s 1-m wireless link with an EVM of 17% at 230 GHz in an SiGe technology," *IEEE Microw. Wireless Compon. Lett.*, vol. 29, no. 4, pp. 297–299, Apr. 2019.
- [173] M. Elkhoully, S. Glisic, C. Meliani, F. Ellinger, and J. C. Scheytt, "220–250-GHz phased-array circuits in 0.13- μm SiGe BiCMOS technology," *IEEE Trans. Microw. Theory Techn.*, vol. 61, no. 8, pp. 3115–3127, Aug. 2013.
- [174] D. Knoll *et al.*, "BiCMOS silicon photonics platform for fabrication of high-bandwidth electronic-photonics integrated circuits," in *Proc. IEEE 16th Top. Meeting Silicon Monolithic Integr. Circuits RF Syst.*, Austin, TX, USA, Jan. 2016, pp. 46–49.
- [175] A. Güner, T. Mausolf, J. Wessel, D. Kissinger, and K. Schmalz, "A 440–540 GHz sub-harmonic mixer in 130 nm SiGe BiCMOS," *IEEE Microw. Wireless Compon. Lett.*, vol. 30, no. 12, pp. 1161–1164, Dec. 2020.
- [176] A. Güner, T. Mausolf, J. Wessel, D. Kissinger, and K. Schmalz, "A 440–540 GHz transmitter in 130 nm SiGe BiCMOS technology," *IEEE Microw. Wireless Compon. Lett.*, vol. 31, no. 6, pp. 779–782, Jun. 2021.
- [177] R. Jain, P. Hillger, E. Ashna, J. Grzyb, and U. R. Pfeiffer, "A 64-pixel 0.42-THz source SoC with spatial modulation diversity for computational imaging," *IEEE J. Solid-State Circuits*, vol. 55, no. 12, pp. 3281–3293, Dec. 2020.
- [178] R. Lachner, "Towards 0.7 terahertz silicon germanium heterojunction bipolar technology—The DOTSEVEN project (invited)," *ECS Trans.*, vol. 64, no. 6, pp. 21–37, Aug. 2014.
- [179] (2017). *Towards Advanced BiCMOS Nanotechnology Platforms for RF and THz Applications (TARANTO)*. [Online]. Available: <https://cordis.europa.eu/project/id/737454>
- [180] D. Knoll *et al.*, "Substrate design and thermal budget tuning for integration of photonic components in a high-performance SiGe:C BiCMOS process," *ECS Trans.*, vol. 50, no. 9, pp. 297–303, Mar. 2013.
- [181] A. Awny *et al.*, "A 40 Gb/s monolithically integrated linear photonic receiver in a 0.25- μm BiCMOS SiGe:C technology," *IEEE Microw. Wireless Compon. Lett.*, vol. 25, no. 7, pp. 469–471, Jul. 2015.
- [182] M. H. Eissa *et al.*, "A wideband monolithically integrated photonic receiver in 0.25- μm SiGe:C BiCMOS technology," in *Proc. Eur. Solid-State Circuits Conf.*, Lausanne, Switzerland, Sep. 2016, pp. 487–490.
- [183] P. Rito *et al.*, "A monolithically integrated segmented linear driver and modulator in EPIC 0.25- μm SiGe:C BiCMOS platform," *IEEE Trans. Microw. Theory Techn.*, vol. 64, no. 12, pp. 4561–4572, Dec. 2016.
- [184] G. Dziallas, A. Fatemi, A. Malignaggi, and G. Kahmen, "A monolithic-integrated broadband low-noise optical receiver with automatic gain control in 0.25 μm SiGe BiCMOS," in *IEEE Top. Meeting Silicon Monolithic Integr. Circuits RF Syst. Dig.*, San Diego, CA, USA, Jan. 2021, pp. 1–3.
- [185] P. Steglich, S. Bondarenko, C. Mai, M. Paul, M. G. Weller, and A. Mai, "CMOS-compatible silicon photonic sensor for refractive index sensing using local back-side release," *IEEE Photon. Technol. Lett.*, vol. 32, no. 19, pp. 1241–1244, Oct. 2020.
- [186] P. Steglich *et al.*, "Hybrid-waveguide ring resonator for biochemical sensing," *IEEE Sensors J.*, vol. 17, no. 15, pp. 4781–4790, Aug. 2017.
- [187] S. Lischke *et al.*, "Ge photodiode with -3dB OE bandwidth of 110 GHz for PIC and ePIC platforms," in *IEDM Tech. Dig.*, San Francisco, CA, USA, Dec. 2020, pp. 1–4.
- [188] A. Rahim, T. Spuesens, R. Baets, and W. Bogaerts, "Open-access silicon photonics: Current status and emerging initiatives," *Proc. IEEE*, vol. 106, no. 12, pp. 2313–2330, Dec. 2018.
- [189] K. Giewont *et al.*, "300-mm monolithic silicon photonics foundry technology," *IEEE J. Sel. Topics Quantum Electron.*, vol. 25, no. 5, pp. 1–11, Sep. 2019.

- [190] M. Rakowski *et al.*, “45 nm CMOS—Silicon photonics monolithic technology (45CLO) for next-generation, low power and high speed optical interconnects,” in *Proc. Opt. Fiber Commun. Conf.*, San Diego, CA, USA, Mar. 2020, pp. 1–3.
- [191] N. G. Weimann *et al.*, “SciFab—A wafer-level heterointegrated InP DHBt/SiGe BiCMOS foundry process for mm-wave applications,” *Phys. Status Solidi A*, vol. 213, no. 4, pp. 909–916, Jan. 2016.
- [192] M. Hossain *et al.*, “A hetero-integrated W-band transmitter module in InP-on-BiCMOS technology,” in *Proc. 13th Eur. Microw. Integr. Circuits Conf. (EuMIC)*, Madrid, Spain, Sep. 2018, pp. 97–100.
- [193] A. Gutierrez-Aitken *et al.*, “A meeting of materials: Integrating diverse semiconductor technologies for improved performance at lower cost,” *IEEE Microw. Mag.*, vol. 18, no. 2, pp. 60–73, Mar. 2017.
- [194] H. Theuss, C. Geissler, and W. Hartner, “Trends in fan out wafer level packaging,” in *Proc. Int. Conf. Adv. Semicond. Devices Microsyst.*, Smolenice, Slovakia, Oct. 2020, pp. 106–110.
- [195] M. Wietstruck, S. Marschmeyer, C. Wipf, M. Stocchi, and M. Kaynak, “BiCMOS through-silicon via (TSV) signal transition at 240/300 GHz for mm-wave sub-THz packaging and heterogeneous integration,” in *Proc. Eur. Microw. Conf.*, Utrecht, The Netherlands, Jan. 2021, pp. 244–247.
- [196] S. Monayakul *et al.*, “Flip-chip interconnects for 250 GHz modules,” *IEEE Microw. Wireless Compon. Lett.*, vol. 25, no. 6, pp. 358–360, Jun. 2015.
- [197] N. G. Weimann *et al.*, “Manufacturable low-cost flip-chip mounting technology for 300–500-GHz assemblies,” *IEEE Trans. Compon., Packag., Manuf. Technol.*, vol. 7, no. 4, pp. 494–501, Apr. 2017.
- [198] R. L. Schmid, A. Ç. Ulusoy, S. Zeinolabedinzadeh, and J. D. Cressler, “A comparison of the degradation in RF performance due to device interconnects in advanced SiGe HBT and CMOS technologies,” *IEEE Trans. Electron Devices*, vol. 62, no. 6, pp. 1803–1810, Jun. 2015.
- [199] T. Brandtner, K. Pressel, N. Floman, M. Schultz, and M. Vogl, “Chip/package/board co-design methodology applied to full-custom heterogeneous integration,” in *Proc. IEEE 70th Electron. Compon. Technol. Conf. (ECTC)*, Jun. 2020, pp. 1718–1727.
- [200] G. Kahmen, “Requirements, design flow and use of FOWLP technology in high performance mixed signal ASICs for test and measurement applications,” in *Proc. Workshop, Fan-Out Wafer Level 3D Packag. Technol. RF mm-Wave Appl.*, Eur. Microw. Conf., Nuremberg, Germany, Oct. 2017.
- [201] X. Gu, D. Liu, and B. Sadhu, “Packaging and antenna integration for silicon-based millimeter-wave phased arrays: 5G and beyond,” *IEEE J. Microw.*, vol. 1, no. 1, pp. 123–134, Jan. 2021.
- [202] T. Sowlatiet *et al.*, “A 60-GHz 144-element phased-array transceiver for backhaul application,” *IEEE J. Solid-State Circuits*, vol. 53, no. 12, pp. 3640–3659, Dec. 2018.
- [203] V. Giannini *et al.*, “A 79 GHz phase-modulated 4 GHz-BW CW radar transmitter in 28 nm CMOS,” *IEEE J. Solid-State Circuits*, vol. 49, no. 12, pp. 2925–2937, Dec. 2014.
- [204] Y. Tousei and E. Afshari, “A high-power and scalable 2-D phased array for terahertz CMOS integrated systems,” *IEEE J. Solid-State Circuits*, vol. 50, no. 2, pp. 597–609, Feb. 2015.
- [205] H. Saeidi, S. Venkatesh, C. R. Chappidi, T. Sharma, C. Zhu, and K. Sengupta, “A 4×4 distributed multi-layer oscillator network for harmonic injection and THz beamforming with 14 dBm EIRP at 416 GHz in a lensless 65 nm CMOS IC,” in *IEEE Int. Solid-State Circuits Conf. (ISSCC) Dig. Tech. Papers*, San Francisco, CA, USA, Feb. 2020, pp. 256–258.
- [206] H. Jalili and O. Momeni, “A 0.46-THz 25-element scalable and wide-band radiator array with optimized lens integration in 65-nm CMOS,” *IEEE J. Solid-State Circuits*, vol. 55, no. 9, pp. 2387–2400, Sep. 2020.
- [207] Y. Yang, O. D. Gurbuz, and G. M. Rebeiz, “An eight-element 370–410-GHz phased-array transmitter in 45-nm CMOS SOI with peak EIRP of 8–8.5 dBm,” *IEEE Trans. Microw. Theory Techn.*, vol. 64, no. 12, pp. 4241–4249, Dec. 2016.
- [208] K. Takano *et al.*, “A 105 Gb/s 300 GHz CMOS transmitter,” in *IEEE Int. Solid-State Circuits Conf. (ISSCC) Dig. Tech. Papers*, San Francisco, CA, USA, Feb. 2017, pp. 308–309.
- [209] S. Lee *et al.*, “An 80-Gb/s 300-GHz-band single-chip CMOS transceiver,” *IEEE J. Solid-State Circuits*, vol. 54, no. 12, pp. 3577–3588, Dec. 2019.
- [210] I. Abdo *et al.*, “A 300 GHz-band phased-array transceiver using bi-directional outphasing and Hartley architecture in 65 nm CMOS,” in *IEEE Int. Solid-State Circuits Conf. (ISSCC) Dig. Tech. Papers*, San Francisco, CA, USA, Feb. 2021, pp. 316–318.



Dietmar Kissinger (Senior Member, IEEE) received the Dipl.Ing., Dr.Ing., and habil. degrees in electrical engineering from FAU Erlangen-Nürnberg, Erlangen, Germany, in 2007, 2011, and 2014, respectively.

From 2007 to 2010, he was with Danube Integrated Circuit Engineering, Linz, Austria, where he worked as a System and Application Engineer at the Automotive Radar Group. From 2010 to 2014, he held a position as a Lecturer and the Head of the Radio Frequency Integrated Sensors Group, Institute for Electronics Engineering, Erlangen. From 2015 to 2018, he was with the Technische Universität Berlin, Berlin, Germany, and the Head of the Circuit Design Department, IHP, Frankfurt (Oder), Germany. Since 2019, he has been a Full Professor for High-Frequency Circuit Design at Ulm University, Ulm, Germany, and the Head of the Institute of Electronic Devices and Circuits. He has authored or coauthored over 350 technical articles and holds more than ten patents. His current research interests include silicon high-frequency and high-speed integrated circuits and systems for communication and automotive, industrial, security, and biomedical sensing applications.

Dr. Kissinger is also a member of the European Microwave Association (EuMA) and the German Association of Electrical Engineers (VDE). He is also an elected member of the IEEE MTT-S Administrative Committee. He received the 2017 IEEE MTT-S Outstanding Young Engineer Award, the 2017 VDE/VDI GMM-Prize, and the 2018 VDE ITG-Prize. He was a co-recipient of over ten best paper awards. He also serves as the Chair for the IEEE MTT-S Technical Coordination and Future Directions Committee, a member of the Technical Program Committee for the European Solid-State Circuits Conference (ESSCIRC), and the TPC Chair for the 2022 German Microwave Conference (GeMic). He was a two-time Chair of the IEEE Topical Conference on Wireless Sensors and Sensor Networks (WiSNet) and a two-time Chair of the IEEE Topical Conference on Biomedical Wireless Technologies, Networks and Sensing Systems (BioWireless). He served as a member of the 2013 and 2017 European Microwave Week (EuMW) Organizing Committee and the 2018 IEEE MTT-S International Microwave Symposium (IMS) Steering Committee and the Executive Committee Chair for the Radio and Wireless Week (RWW). He was a nine-time Guest Editor for the *IEEE Microwave Magazine*. He served as an Associate Editor for the IEEE TRANSACTIONS ON MICROWAVE THEORY AND TECHNIQUES. He was the Chair of the IEEE MTT-S Technical Committee on Microwave and Millimeter-Wave Integrated Circuits (MTT-14).



Gerhard Kahmen (Senior Member, IEEE) received the Dipl.Ing. degree in electrical engineering from RWTH Aachen, Aachen, Germany, in 1997, and the Dr.Ing. degree in electrical engineering from Ulm University, Ulm, Germany, in 2016.

From 1998 to 2000, he worked at Philips Semiconductors, Nijmegen, The Netherlands, on power amplifier modules for handsets. In 2001, he joined the Test and Measurement Division, Rohde & Schwarz, Munich, Germany, where he developed high-dynamic-range broadband RF mixed-signal application-specific integrated circuits (ASICs) for test and measurement equipment. From 2006 to 2010, he was leading the Mixed-Signal ASIC Research and Development Team as the Director of engineering being directly involved in the development of key ASIC components for Rohde & Schwarz equipment. From 2011 to 2019, he was responsible for the worldwide mixed-signal ASIC research and development activities of Rohde & Schwarz in a Vice President position, including a research and development site in Portland, OR, USA. Within this appointment, he was directly involved in the development of complex mixed-signal systems, such as high-dynamic-range GS/s Nyquist rate digital-to-analog converters (DACs) for digital RF signal generation and analog-to-digital converters (ADCs) for digital oscilloscopes. Since 2020, he has been the Chief Executive Officer of IHP—Leibniz Institute for High Performance Microelectronics, Frankfurt (Oder), Germany. He holds a full professorship for semiconductor technology at Brandenburg Technical University (BTU), Cottbus, Germany. His research interests are broadband RF/mixed-signal ASICs with high dynamic range, ultrahigh-speed digital-to-analog/analog-to-digital converters for digital RF signal generation and analysis, Si-photonic RF ASICs, and technologies for heterointegration of complex RF/mixed-signal systems.



Robert Weigel (Fellow, IEEE) was born in Ebermannstadt, Germany, in 1956. He received the Dr.Ing. and Dr.Ing. habil. degrees in electrical engineering and computer science from the Munich University of Technology, Munich, Germany, in 1989 and 1992, respectively.

He has been a Professor of RF circuits and systems at the Munich University of Technology from 1994 to 1996. From 1996 to 2002, he was a Full Professor and the Director of the Institute for Communications and Information Engineering, University of Linz, Linz, Austria. In Linz, in August 1999, he co-founded the company DICE, Linz, meanwhile split into an Infineon Technologies company (DICE) and an Apple company [in between an Intel company (DMCE)], which are devoted to the design of integrated circuits and systems with over 700 coworkers. Since 2002, he has been a Full Professor and the Director of the Institute for Electronics Engineering, Friedrich-Alexander-University of Erlangen-Nuremberg, Erlangen, Germany. In 2012, he co-founded the company eesy-ic, Erlangen, devoted to RF and mixed-signal circuits, with meanwhile over 60 staff members. He has been engaged in research and development of microwave theory and techniques, electronic circuits and

systems, and communication and sensing systems. In these fields, he has published about 1350 articles and a number of patents.

Dr. Weigel is a Fellow of the German ITG and an elected member of the German National Academy of Science and Engineering (acatech). He has been an elected member of the Senate of the German Research Foundation (DFG). He has been a member of numerous conference steering and technical program committees. He received the 2002 VDE ITG-Award, the 2007 IEEE Microwave Applications Award, the 2016 IEEE MTT-S Distinguished Educator Award, the 2018 Distinguished Service Award of the EuMA, the 2018 IEEE Rudolf Henning Distinguished Mentoring Award, and the 2020 IEEE Microwave Career Award. He was the General Chair of several conferences, such as the 2013 European Microwave Week in Nuremberg, Germany, and the Technical Program Chair of several conferences, such as the 2002 IEEE International Ultrasonics Symposium in Munich, Germany, and the 2003 and 2007 EuMA European Conferences on Wireless Technology, Munich. He served in many roles for the IEEE Microwave Theory and Techniques (MTT) and Ultrasonics, Ferroelectrics, and Frequency Control (UFFC) Societies. He has been Founding Chair of the Austrian COM/MTT Joint Chapter, a Region 8 MTT-S Coordinator, a Distinguished Microwave Lecturer, an MTT-S AdCom Member, and the 2014 IEEE MTT-S President.